TODD, DANIEL A., Ph.D. Exploration of Quorum Sensing Inhibition in Gram Positive Bacterial Pathogens Using Mass Spectrometry. (2015)
Directed by Dr. Nadja B Cech. 71 pp.

Antibiotics have been used as the primary treatment for bacterial infections since the 1940's. Unfortunately, the use and misuse of antibiotics has led to the proliferation of antibiotic-resistant bacteria and resulted in the loss of antibiotic efficacy. Alternative strategies for fighting bacterial infections are needed to preserve our ability to cure bacterial infections. One strategy that has shown promise in *in vitro* and animal studies is the anti-virulence approach. Unlike the traditional antibiotic approach, which focuses on inhibiting bacterial growth, the anti-virulence approach focuses on disrupting bacteria pathogenesis. Inhibition of bacteria pathogenesis results in a less invasive infection that can be cleared by the innate immune system. Anti-virulence compounds have proven to be less susceptible to resistance development, which suggests their potential for long term therapeutic development. Unfortunately, only a limited number of anti-virulence compounds have been discovered and none have made it to the clinical setting. One goal of this research was to develop a new biological screening method to identify new anti-virulence compounds, particularly aimed at treating Gram-positive bacterial infections.

In Gram-positive bacteria such as *Staphylococcus aureus*, virulence is regulated by the accessory gene regulator (*agr*) system. The *agr* system is a quorum sensing system activated by a small cyclic peptide known as AIP. The inhibition of the quorum sensing system results in the inhibition of bacterial virulence, making this system an ideal target for anti-virulent therapeutics. With this research, we developed a liquid chromatography-mass spectrometry (LC-MS) method to measure the activity of potential

quorum sensing inhibitors based on their ability to inhibit AIP production. Prior to applying this method, it was necessary to develop approaches to detect the AIPs of interest directly from bacterial cultures, and to elucidate the structures of unknown AIPs. Mass spectrometry was employed to achieve both of these goals, and we detected eight AIPs directly from bacterial cultures. In addition, we elucidated the structures of two previously unidentified AIPs, that of *Listeria monocytogenes* and *Staphylococcus saprophyticus.* The newly developed assay was then utilized to identify a new quorum sensing inhibitor, 8-oxotetrahydrothalifendine, which was shown to act as a quorum sensing signal biosynthesis inhibitor in *Staphylococcus aureus*. Future experiments will involve employing the newly developed assay to screen natural product extract libraries for novel quorum sensing inhibitors.

# EXPLORATION OF QUORUM SENSING INHIBITION IN GRAM POSITIVE BACTERIAL PATHOGENS USING MASS SPECTROMETRY

by

Daniel A. Todd

A Dissertation Submitted to
the Faculty of the Graduate School at
The University of North Carolina at Greensboro
in Partial Fulfillment
of the Requirements for the Degree
Doctor of Philosophy

Greensboro
2015

Approved by

_____
Committee Chair

To my wife, Jessi, for her continual support and inspiration, and daughter, Addilynn, for her much needed, and sometimes underappreciated, distractions. I could not have done it without you.

APPROVAL PAGE

This dissertation written by Daniel A. Todd has been approved by the following committee of Faculty of the Graduate School at The University of North Carolina at Greensboro.

Committee Chair _____

Committee Members _____

_____

_____

_____
Date of Acceptance by Committee

_____
Date of Final Oral Examination

# ACKNOWLEDGMENTS

The National Center for Complementary and Integrative Health (R01 AT006860), for providing financial support for this project

Dr. Hiyas Junio and Dr. Vamsikrishna Kandhi, for providing training and support during the early stages of this project

Dr. Brandie Ehrmann, for providing mass spectrometry training and advice

Dr. Nicholas Oberlies, for allowing me access to his equipment and instrumentation, and providing valuable insight into experimental design

Dr. Alexander Horswill, for providing all the bacterial strains used in this study, opening up his laboratory to me, and providing valuable advice and insight into the microbiology utilized in this project

Dr. Nadja Cech, for providing me the opportunity to conduct this research and the funding that supported it, and for her endless advice and support

TABLE OF CONTENTS

Page

LIST OF TABLE ..... vii

LIST OF FIGURES ..... viii

CHAPTER

I. A BRIEF HISTORY OF ANTIBIOTICS, THE DEVELOPMENT OF ANTIBIOTIC RESISTANCE, AND HOPE FOR THE FUTURE ..... 1

1.1 History of Antibiotics ..... 1
1.1.1 The Dawning of the Antibiotic Era ..... 1
1.1.2 The Golden Age of Antibiotics ..... 3
1.1.3 The Current Void ..... 5
1.2 Antibiotic Resistance – The End of the Miracle Cure ..... 6
1.2.1 Foundations of Resistance ..... 6
1.2.2 Mechanisms of Resistance ..... 8
1.3 Looking to the Future ..... 11

II. IDENTIFICATION AND QUANTIFICATION OF AUTO-INDUCING PEPTIDES ..... 13

2.1 Introduction ..... 13
2.2 Materials and Methods ..... 18
2.2.1 Instrumentation ..... 18
2.2.2 Bacterial Strains, Media and Growth Conditions ..... 18
2.2.3 Identification and Detection of Auto-Inducing Peptides ..... 19
2.2.3.1 Confirmation of *Listeria monocytogenes* AIP ..... 20
2.2.3.2 Confirmation of *Staphylococcus saprophyticus* AIP ..... 20
2.2.4 Ambuic Acid Inhibition Assays ..... 21
2.3 Results ..... 21
2.3.1 Identification of AIPs ..... 21
2.3.2 Quantification of AIP ..... 25
2.3.3 Broad Applicability of Ambuic Acid as a Quorum Sensing Inhibitor ..... 28
2.3.4 Growth Effects ..... 29
2.4 Discussion ..... 31
2.5 Conclusion ..... 32

III. DEVELOPMENT OF A BIOASSAY TARGETING AIP BIOSYNTHESIS ..... 33

3.1 Introduction ..... 33
3.2 Materials and Methods ..... 35
3.2.1 Instrumentation ..... 35
3.2.2 Bacterial Strains, Media and Growth Conditions ..... 36
3.2.3 Engineering of AIP Constitutively Producing Strain (AH2989) ..... 36
3.2.4 Pure Compounds for Screening ..... 37
3.2.5 Screening for AIP Biosynthesis Inhibitors ..... 37
3.2.6 Quantification of AIP ..... 38
3.3 Results ..... 39
3.3.1 Development of Targeted Bioassay ..... 39
3.3.2 Confirmation of Ambuic Acid's Mode of Action ..... 41
3.3.3 Growth Inhibition ..... 42
3.3.4 Natural Product Compound Screening ..... 44
3.4 Discussion ..... 47
3.5 Conclusion ..... 48

IV. INDENTIFICATION OF AN AIP BIOSYNTHESIS INHIBITOR IN GOLDENSEAL (*HYDRASTIS CANADENSIS*) LEAF EXTRACT ..... 49

4.1 Introduction ..... 49
4.2 Materials and Methods ..... 51
4.2.1 Preparation of a Goldenseal Extract ..... 51
4.2.2 Fractionation of Goldenseal Extract ..... 51
4.2.2.1 Stages 1 and 2 of Separation ..... 51
4.2.2.2 Stage 3 of Separation ..... 52
4.2.2.3 Preparative HPLC ..... 52
4.2.3 Identification of 8-Oxotetrahydrothalifendine ..... 53
4.2.4 AIP Biosynthesis Inhibition Assay ..... 54
4.3 Results ..... 54
4.4 Discussion ..... 60
4.5 Conclusion ..... 61

V. CONCLUDING THOUGHTS AND COMMENTS ..... 62

REFERENCES ..... 64

LIST OF TABLES

Page

Table 1. Bacteria Species Containing *Agr* Systems ..... 17

Table 2. Bacteria Strains ..... 19

Table 3. $IC_{50}$ Values for Ambuic Acid Inhibition of AIP Biosynthesis ..... 29

Table 4. Bacteria Strains ..... 36

Table 5. Comparison of Experimental and Literature NMR Values for 8-Oxotetrahydrothalifendine ..... 59

LIST OF FIGURES

Page

Figure 1. Timeline of Antibiotic Introduction and the Identification of Resistance ..... 7

Figure 2. Structure of Penicillin ..... 9

Figure 3. Structure of Methicillin ..... 10

Figure 4. Schematic of the *Agr* System ..... 15

Figure 5. Identification of *Listeria monocytogenes* AIP ..... 23

Figure 6. Identification of *Staphylococcus saphrophyticus* AIP ..... 24

Figure 7. Inhibition of *S. aureus Agr* System ..... 26

Figure 8. Inhibition of AIP Production by MRSA (AH1263) with Ambuic Acid ..... 27

Figure 9. Dose-Response Curve for Ambuic Acid ..... 28

Figure 10. Growth Curve for *S. aureus Agr* Type I with Ambuic Acid ..... 30

Figure 11. Bioassay Workflow ..... 40

Figure 12. Comparison of *Agr* System Inhibition ..... 42

Figure 13. Example of Growth Inhibition ..... 43

Figure 14. Example of Growth Delay ..... 44

Figure 15. Example of Endpoint Analysis ..... 45

Figure 16. Growth Curves for Lead Compounds ..... 46

Figure 17. Evaluation of Acremonidin C ..... 47

Figure 18. Overview of Bioactivity-Directed Fractionation ..... 50

Figure 19. Bioactivity of Fractions i-xii ..... 55

Figure 20. Bioactivity of Fractions a-aa ..... 56

Figure 21. Confirmation of 8-Oxotetrahydrothalifendine in Fractions ..... 58

Figure 22. Bioactivity of 8-Oxotetrahydrothalifendine ..... 60

# CHAPTER I

# A BRIEF HISTORY OF ANTIBIOTICS, THE DEVELOPMENT OF ANTIBIOTIC RESISTANCE, AND HOPE FOR THE FUTURE

## 1.1 History of Antibiotics

The commercialization of antibiotics was undoubtedly one of the greatest advancements of modern medicine [1]. These powerful therapeutic agents has saved countless lives throughout history, and forever changed our approach to treating microbial infections. In this brief summary, we will discuss the key events in science history that helped bring about the dawning antibiotic era, explore the promise of the "Golden Age" of antibiotic drug discovery, and investigate recent decades of discovery void.

### 1.1.1 The Dawning of the Antibiotic Era

The existence of bacteria was first recognized in the late 1600's [2]. However, it was not until two centuries later that the connection between bacteria and disease was observed [2, 3]. Bacteria have since been associated with some of the worst epidemics in human history, including the bubonic plague, syphilis and tuberculosis [3]. Mankind has spent an immense amount of time and resources attempting to combat these deadly infectious, and up until the early 1900's a majority of the progress made was due to preventative measures [3]. In 1909, Paul Ehrlich discovered the first antimicrobial

agent used specifically to cure a bacterial infection. Ehrlich is accredited for discovering the drug salvarsan, a highly effective treatment for syphilis. Prior to this discovery, syphilis was recognized as incurable, epidemic disease that was highly prevalent in Europe and North America starting the in late 1400's. While salvarsan's mode of action is still unknown, it was the most frequently prescribed drug up to the 1940's and laid the ground work for discovery of new antimicrobials.

Another early antimicrobial that helped to usher in the antibiotic era was the sulfanilamide drug prontosil [1]. Prontosil was first synthesized by two chemists at Bayer, Josef Klarer and Fritz Mietzsch [1] in 1935, and was identified by Gerhard Domagk as a treatment for a number of diseases. Once the effectiveness of this class of compounds to fight bacterial infections was observed, several derivatives became available [1]. Sulfanilamides proved to be an effective treatment for a variety of bacterial infections, including the streptococcal infections commonly associated with burns and childbirth in the late 1800's [2]. One report in 1846 put the maternal mortality rate at 11.4% for women delivering in the maternity ward of a prominent clinic in Vienna. While changes in general hygiene helped reduced this number down to 3%, it was until the introduction of sulfanilamide drugs that this number became much more on par with today's standards of <0.02%. Following the introduction of sulfanilamides the mortality rate of acute meningococcal meningitis decreased from 70-90% to approximately 10% [4].

While salvarsan and protosil both played significant roles leading to the development of modern antibiotic treats, Penicillin is the most widely recognized as the

drug that began the antibiotic era. In 1928, Alexander Fleming observed that a colony of *Penicillium rubrum* was capable of causing co-cultured *Staphlyococcus* cells to lyse [5]. He further went on to investigate the antibacterial characteristics of the *P. rubrum* filtrate, and discovered it was very potent against a variety of bacteria [5]. Fleming spent the following decade attempting to isolate the compound responsible for the observed antibacterial activity. However, his efforts were unsuccessful [1]. Fortunately, in 1940, Howard Florey and Ernest Chain developed a method for purifying penicillin in significant quantities and showed its efficacy with *in vivo* studies [6]. Penicillin was successfully used for the first time United States in 1942 [7], and by 1945, over 650 billion units of penicillin were being produced monthly [7]. Penicillin quickly surpassed salvarsan as the most frequently prescribed drug [1], and has been attributed to saving over 2 million lives during World War II.

For their significant contributions to society Ehrlich, Domagk, Fleming, Florey, and Chain were all award Nobel Prizes in Physiology or Medicine. Ehrlich received the 1908 Nobel Prize, Domagk was award the 1939 Nobel Prize, and Fleming, Florey, and Chain received the 1945 Nobel Prize [8]. Each of these key discoveries played a crucial role in laying the groundwork for the antibiotic era and was responsible for saving countless lives throughout history.

### 1.1.2 The Golden Age of Antibiotics

The promise brought about by the discovery of the first antibiotics led to a surge of research effort into discovery of new antimicrobial compounds. The time period between the 1940's and the early 1970's saw the greatest increase of new classes of

antibiotics in history, therefore has been dubbed the "Golden Age" of antibiotic discovery. This section is dedicated to exploring some of the key discoveries made during this time-period.

The discoveries of salvarsan, protosil, and penicillin not only provided promise the bacterial infections could be efficiently cured, but also provided the basic framework for discovering new antibiotics. After learning of Fleming's serendipitous discovery of penicillin from a *P. rubrum* fungal isolate, Selman Abraham Waksman turned to *Actinomycetes* cultures hoping to discover antibiotics that were even more promising. This decision paid off in the early 1940's, when Waksman and his student, Albert Schatz, discovered streptomycin. Streptomycin was a new class of antibiotic, capable of inhibiting the growth of both Gram-positive and Gram-negative pathogens [9]. The most interesting activity of streptomycin was its ability to fight tuberculosis infections.

During the 1880's, tuberculosis was responsible for one in five deaths in England, and by 1937 it was the leading cause of death in the United States. In 1945 streptomycin delivered on its promise as a cure for this deadly infection, and cured its first patient with a pulmonary tuberculosis infection. While streptomycin is most notably recognized for its success against tuberculosis, it was also an effective treatment for a number of other diseases including: leprosy, meningitis, empyema, pneumonia, gonorrhea, tularaemia and glanders [10]. For the discovery of streptomycin, Waksman was award the 1952 Nobel Prize for Physiology and Medicine [8].

The first broad-spectrum antibiotic identified was chloramphenicol. This antibiotic was originally isolated from *Streptomycin venezuelea* by Paul Burkholder, but

became the first antibiotic to be fully synthesized [10, 11]. Chloramphenicol was most widely recognized for its ability to cure typhus, an infection caused by *Rickettsia prowazeki* [12]. This devastating disease can be found worldwide and has been responsible for a number of epidemics throughout history [12]. The success of chloramphenicol was soon overshadowed by its devastating side effects and its use began to drop drastically. Fortunately, by this time Benjamin Duggar had identified aureomycin, the second antibiotic with broad-spectrum capabilities. Aureomycin proved to be an effective treatment of typhus without the life threatening side effects.

The time period between 1940 and 1970 brought about the discovery of 12 new classes of antibiotics [4] and provided hope for those suffering from bacterial infections. Some of the other key discoveries during this time include: erythromycin (1952), vancomycin (1956) and genamicin (1963) [10]. Unfortunately, the introduction of trimethoprim in 1968 proved to be the end of the Golden Age, and no new classes of antibiotics were introduced until the year 2000 [4, 13].

### 1.1.3 The Current Void

Changes in regulation and decreasing interest in antibiotics by the pharmaceutical industry have led to reduced antibiotic innovation. A recent review by Lynn Silver accentuates this problem by pointing out that though we have recently introduced new classes of antibiotics to the market, these classes were all discovered decades earlier and no new class of antibiotic has been discovered since 1987 [14]. The lack of new antibiotic classes, however, does not mean a lack in new therapeutic agents. There has been a continuing flow of new antibiotics introduced since the 1970's, however, these

have all been members of previously identified classes or modifications of existing therapeutics [1]. Unfortunately, this pipeline, too, has become depleted. Between the1983 and 2002 there was 56% drop in new antibiotics approved by the Food and Drug Administration [4].

## 1.2 Antibiotic Resistance - The End of the Miracle Cure

During his Nobel lecture in 1945, Alexander Fleming forewarned that improper use of penicillin could result in penicillin-resistant bacteria [8]. Over half a century later, resistance has been discovered to every major class of antibiotic (Figure 1). In 2013, the Centers for Disease Control and Prevention (CDC) released a report on the threat of antibiotic resistance that revealed over 2 million illnesses are a direct result of antibiotic resistant microorganisms in the United States each year. This report also indicated that over 23,000 deaths occur each year in the United States attributable to these threats. This section will discuss some of the factors that have resulted in the current antibiotic resistant epidemic and explore some the mechanism of resistance utilized by bacteria.

### 1.2.1 Foundations of Resistance

The misuse of antibiotics plays a role in current antibiotic resistance epidemic. In 2008, it was estimated that over 55% of all the antibiotics prescribed for acute respiratory infections in the United States were unnecessary [15]. The majority of these infections are viral, not bacterial, and therefore are unaffected by the use of antibiotics [16]. When a patient is given unnecessary antibiotics, their natural microflora can adapt to the presence of the antibiotic and establish resistance. If the patient then develops an actual bacterial infection, the resistance genes can be transferred to the pathogen, resulting in an

antibiotic resistant bacteria pathogen. While healthcare professionals may be responsible for prescribing unnecessary antibiotics, patients have also attributed to the rise in antibiotic resistance by not proper taking antibiotics that have been appropriately prescribed. When a patient takes the incorrect dose, misses a dose, or prematurely stops treatment, the antibiotic is unable to effectively clear the infection, and the remaining bacteria are exposed to low levels of the antibiotic. This results in the bacterial pathogen surviving long enough to develop a resistance to the antibiotic. In either of the cases described above, the patient can then transfer the antibiotic bacteria to other members within the community, thus perpetuating the problem.

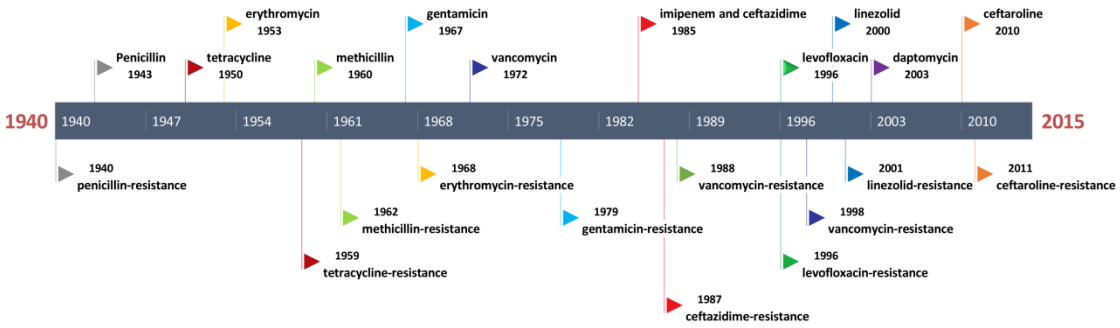


**Figure 1. Timeline of Antibiotic Introduction and the Identification of Resistance.**

Above the timeline shows the year that the antibiotic was introduced for clinical use, and below the timeline shows the year that resistance was identified. Figure is based on a previously published figure by the Centers for Disease Control and Prevention [17].

While the direct misuse of antibiotics have aided in the spread of antibiotic resistance, people can also be exposed to antibiotic resistant bacteria in the food they

consume. In 2011, it was estimated the 80% of the antibiotics sold in the United States went to the agriculture industry [18]. These antibiotics are used primarily for disease management (prevention, treatment, and control) and growth promotion [19]. This overexposure to antibiotics results in the cultivation of antibiotic resistant bacteria in livestock that can be transferred to the human consumer [18, 20-22]. Antibiotics are also excreted by the animals and their manure is then used as fertilizer on crops [23]. This low level of antibiotics results in the development of resistance by plant and soil bacteria [22, 23]. The crops are then harvested for either animal feed [24] or human consummation [18], resulting in the continual spread of antibiotic resistance.

### 1.2.2 Mechanisms of Resistance

There are three primary mechanisms of antibiotic resistance utilized by bacteria: modification of the antibiotic, modification of the target effected by the antibiotic, and removal of the antibiotic from the cell. The modification of the antibiotic typically occurs though enzymatic action. Edward Abraham and Ernest Chain published one of the first records of antibiotic resistance in 1940, two years prior to its first medical use in the United States, in which they noted an enzyme produced by *Balantidium coli* could deactivate penicillin [25]. This was the first of around 1000 β-lactamases enzymes to be identifed [22]. β-lactams, such as penicillin, kill bacterial cells by inhibiting cell wall biosynthesis of the transpeptidase, penicillin-binding protein. The resulting unstable cell wall causes the bacterial cells to lyse. The β-lactam ring (Figure 2) is the primary active site for this class antibiotic. β-lactamases hydrolyze this ring and render the

antibiotic inactive [26]. However, advances in antibiotic research resulted in the development of β-lactams specifically designed to slow down the enzymatic resistance utilized by the bacteria. An example of a β-lactamase resistant antibiotic is methicillin (Figure 3). Unfortunately, within one year after the release of methicillin, methicillin-resistance had been identified [27]. However, this resistance was not a modification of a β-lactamase enzyme, but was a modification of the penicillin-binding protein. Modification of the target protein is the mechanism of resistance utilized by methicillin-resistant *Staphylococcus aureus* [26, 27], one of the most prevalent antibiotic resistant bacteria pathogens in the world. Modification of the penicillin-binding protein structure reduces the affinity of methicillin to the protein and renders methicillin inactive. Modification of the antibiotic or of the antibiotic's target is utilized by a variety of Gram-positive and Gram-negative bacteria as means of antibiotic resistance.

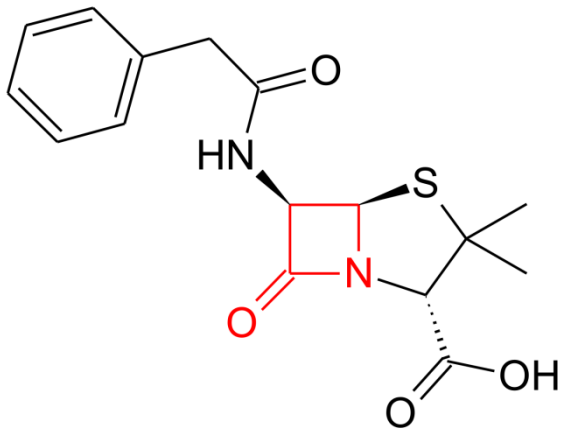


**Figure 2. Structure of Penicillin**

Molecular structure of Penicillin G with the signature β-lactam ring drawn in red. The β-lactam ring is the active site for all antibiotics of the β-lactam class.

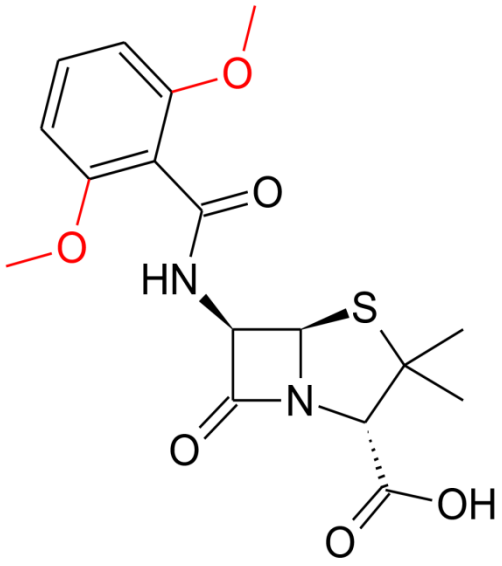


**Figure 3. Structure of Methicillin**

Molecular structure of methicillin with the methoxy groups drawn in red. The addition of the two methoxy groups results in methicillin being less susceptible to β-lactamase modification.

The third mechanism of antibiotic resistance is the removal of the antibiotic from the cell. If the antibiotic is unable to reach a lethal concentration within the cell, the antibiotic will be ineffective at killing the bacteria. The machinery used to remove antibiotics from the cell is known as an efflux pump. There are five families of bacterial efflux pumps: the resistance-nodulation-division (RND) family, the major facilitator superfamily (MFS), the ATP (adenosine triphosphate)-binding cassette (ABC) superfamily, the small multidrug resistance (SMR) family, and the multidrug and toxic compound extrusion (MATE) family [28]. Pumps from the RND, MFS, SMR, and MATE families use an ion exchange force ($H^+$ or $Na^+$) to remove substrates from within

the cell. The ABC family utilizes the hydrolysis of ATP to active the pump [26]. Pumps can either be substrate specific, such as tetracycline pumps, or very generic. This allows for a very broad range of antibiotic resistance [26, 28]. Often times efflux pumps will be over expressed as means of antibiotic resistance, allowing the cell to remove the antibiotic in a more efficient manner. Efflux pumps are found in a variety of Gram-positive and Gram-negative bacteria including *Escherichia coli*, *Neisseria gonorrhoeae*, *Pseudomonas aeruginosa*, *Salmonelle typhimurium*, and *Staphylococcus aureus* [28].

### 1.3 Looking to the Future

The discovery and development of antibiotics has undoubtedly been one the greatest advance in modern medicine, unfortunately it was not without a cost. The rise of antibiotic resistant bacteria has limited the efficacy of once powerful antibiotics, and created an urgent need for the development of novel therapies. While discovering new antibiotics may provide some relief in the current antibiotic resistance epidemic, history shows this may not be a long term solution. Even with good antibiotic stewardship, resistance may be inevitable. In a study conducted by Bhullar *et al.*, antibiotic resistance was identified in a strain of bacteria that had been geographically isolated for 4 million years [29]. Indicating resistance is an inherent characteristic of bacteria, and while misuse of antibiotics may accelerate the predominance of resistance, it is not the root cause.

One approach for combating antibiotic resistant bacteria is combination therapy. This strategy has been successfully utilized to counter β-lactamase resistance with drugs like Augmentin and Primaxin, which combine a β-lactam antibiotic with a β-lactamase

inhibitor. Another combination approach that has proved effective in the laboratory, but has yet to reached the clinic, is the inhibition of bacterial efflux pumps. Inhibition of the efflux pumps would result in the bacteria being unable to remove the antibiotic [30, 31]. While these types of approaches are promising, they still exert selective pressure that leads to the development of resistance. Antibiotics will always play a role in combating bacterial infections, but new strategies for augmenting their use are needed. One option would be to inhibit nonessential bacterial cell function that cause stress to the host. This would allow the host's innate immune system to concentrate its efforts on clearing the bacterial infection, instead of repairing the damage bacteria cause. Inhibition of bacteria pathogenesis is the foundation of the anti-virulence approach that is the focus of the studies presented here. Chapter II is dedicated to understanding ways to inhibit pathogenesis in a variety of Gram-positive bacteria. The knowledge gained by the studies described in Chapter II supports the development of a novel biological assay described in Chapter III, which will permit the efficient screening for new compounds capable of targeting bacterial infections. The efficient screening method is then utilized in Chapter IV to identify a compound from a medicinal plant extract that targets bacterial pathogenesis by an unusual mode of action.

# CHAPTER II

# IDENTIFICATION AND QUANTIFICATION OF AUTO-INDUCING PEPTIDES

## 2.1 Introduction

According to the Centers for Disease Control and Prevention, antibiotic resistant bacteria are responsible for over 2 million illnesses and 23,000 deaths in the United States each year. These infections result in an estimated economic impact of over $55 billion dollars. With an ever-increasing emergence in antibiotic resistance and a depleting antibiotic discovery pipeline, it has become imperative to find new approaches for fighting these costly infections. One promising strategy for combating antibiotic resistant infections is to target bacterial pathogenesis, the so-called "anti-virulence" approach [32]. This strategy has the hypothetical advantages of limiting the evolution of widespread drug resistance, facilitating the development of host immune responses, and avoiding negative impacts on the normal microbial flora [33-36].

In Gram-positive bacteria, virulence is regulated by a quorum sensing system known as the accessory gene regulator (*agr*) system (Figure 4). The *agr* system is activated by a small cyclic peptide known as autoinducing peptide or AIP. The *agr* system has previously been described in detail [37-39]. In short, it consists of four primary components, AgrBDCA. AgrD is a propeptide, which is processed into AIP by the membrane peptidase AgrB and transferred through the cytoplasmic membrane. AIP then binds to the membrane-bound histidine kinase, AgrC, resulting in the

phosphorylation of the AgrA response regulator, which in turn leads to the activation of two RNA promoters P2 and P3. The P2 and P3 promoters activate transcription of RNAII and RNAIII, respectively. RNAII transcription leads to production of AgrBDCA, while RNAIII transcription regulates a variety of cellular functions, including, most importantly, the activation of virulence factors. Each species of bacteria produces a unique *agr* system, and therefore regulated by a unique AIP. Some species of bacteria have developed further diversity and express multiple *agr* types. For example, strains of *S. aureus* are divided into four *agr* types (I, II, III and IV). Each type is activated by a unique AIP (I, II, III and IV).

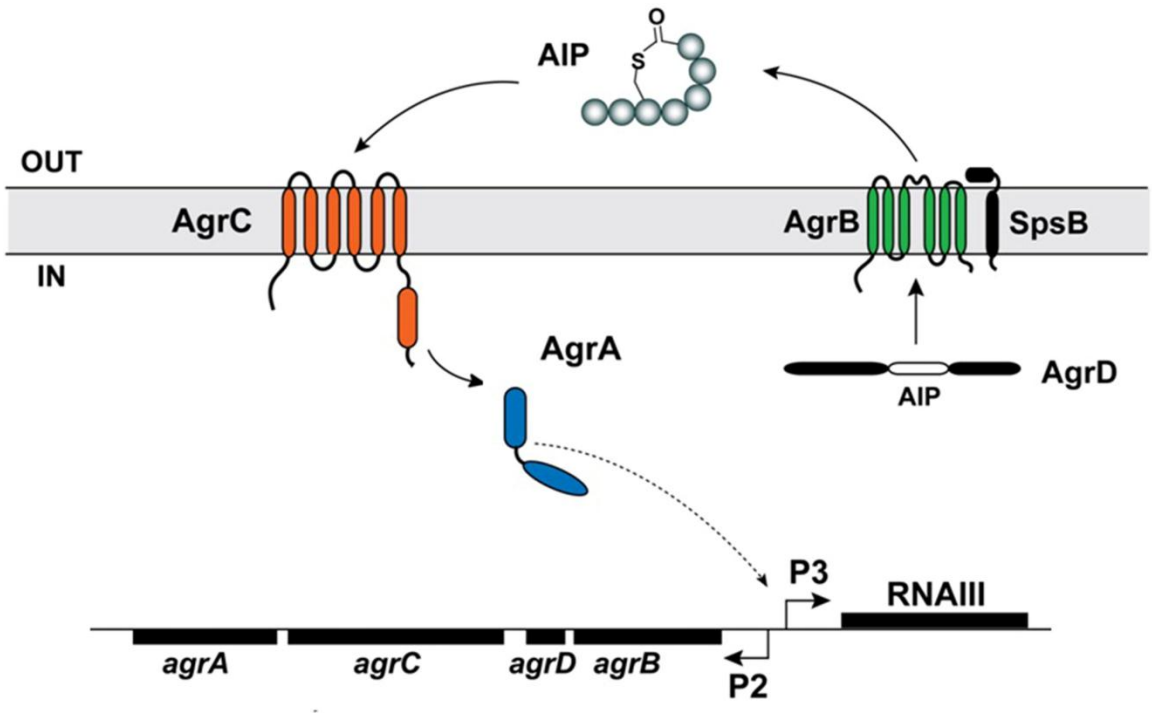


**Figure 4. Schematic of the *Agr* System.**

The *agr* locus is comprised of two divergent transcripts called RNAII and RNAIII driven by the P2 and P3 promoters, respectively [39, 40]. The core machinery of the *agr* system is encoded by the four genes (*agrBDCA*) of the RNAII operon. The propeptide, AgrD, is transformed into the system regulating cyclic peptide, AIP. AIP binds to the AgrC receptor, resulting in the phosphorylation of the AgrA response regulator and the activation of the P2 and P3 promoters [39, 40].

AIP is both an activator of the *agr* system and a direct output. Thus, this molecule is a promising biomarker for monitoring *agr* system activity. If the activity of the *agr* system is reduced, i.e. by the addition of an inhibitor, an associated decrease in AIP production should be observed. An important goal of this study was to develop quantitative approaches for measuring potency of AIP inhibition by relying on detection of AIP.

Until very recently, AIP detection has been a cumbersome task requiring extensive sample cleanup [41-44]. One method was previously developed that allowed direct measurement of AIPs from several species of Gram-positive bacteria using matrix-assisted laser desorption ionization mass spectrometry (MALDI) [45]. However, this approach is inherently limited to qualitative assessments (identification but not quantification). Another approach demonstrated recently by our laboratory could be used to quantify AIP production in bacterial cultures from *Staphylococcus aureus*, which produce AIP at relatively high concentrations (~10 μM) [43, 46]. This method was not, however, effective for identification or quantitative assessments by other bacteria, i.e. *S. epidermidis* and *L. monocytogenes*, presumably because of low levels of AIPs produced by these strains.

Quantitative measurements of AIP production require knowledge of AIP structures; thus, AIP identification was a second goal of this study. The *agr* system genes have been fully sequenced for a number of Gram-positive bacteria [39], and AIP sequences have been predicted for these organisms [39]. However, AIP structures have yet to be confirmed for the majority of Gram-positive bacterial strains (Table 1). A previous study from our laboratory showed that in the case of *S. epidermidis* [44], there was lack of agreement between predicted and measured structures of AIP. Thus, it is important to follow up predictions of AIP structure with experimental verification.

**Table 1. Bacteria Species Containing *Agr* Systems**

| Species | Agr Type | AIP Sequence |
|---|---|---|
| *S. aureus* | I | **YSTCDFIM*** |
| | II | **GGVNACSSLF*** |
| | III | **INCDFLL*** |
| | IV | YSTCYFIM* |
| *S. arlettea* | N/A | VNPCGGWF |
| *S. auricularis* | I | AKTCTVLY |
| | II | TKTCTVLY |
| *S. capitis* | I | ANPCQLYY |
| | II | ANPCALYY |
| *S. caprae* | I | YSTCSYYF |
| | II | YRTCNTYF |
| *S. carnosus* | N/A | YNPCVGYF |
| *S. cohnii cohnii* | N/A | GKVCSAYF |
| *S. cohnii urealyticus* | N/A | VKPCTGFA |
| *S. epidermdis* | I | **DSVCASYF*** |
| | II | **NASKYNPCSNYL*** |
| | III | **NAAKYNPCASYL*** |
| *S. gallinarum* | N/A | ARPCGGFF |
| *S. haemolyticus* | N/A | FTPCTTYF |
| *S. hominis* | N/A | QTVCSGYF |
| *S. intermedius* | N/A | RIPTSTGFF |
| *S. lungdunensis* | I | **DICNAYF*** |
| | II | DMCNGYF |
| *S. pseudintermedius* | I | RIPTSTGFF |
| | II | RIPISTGFF |
| | III | KIPTSTGFF |
| | IV | KYPTSTGFF |

| Species | Agr Type | AIP Sequence |
|---|---|---|
| *S. saphrophyticus* | N/A | **INPCFGYT** |
| *S. simulans* | I | YNPCLGFL |
| | II | YYPCFGYF |
| *S. xylosus* | N/A | AKPCGGFF |
| *S. warneri* | N/A | YSPCTNFF |
| *B. cereus* | N/A | EKLCIGFG |
| *B. halodurans* | N/A | VNASSPLI |
| *B. sphaericus* | N/A | HNFCVLYS |
| *C. acetobutylicum* | N/A | GKCVLVTL |
| *C. beijerincki* | N/A | KCCFSGGL |
| *C. botulinum* | I | SSACYWCV |
| | II | DSACVVGI |
| *C. difficile* | I | NSTCPWII |
| | II | NSASSWVA |
| *C. novyi* | N/A | ACVSLNGL |
| *C. perfringens* | N/A | TSACIWFT |
| *E. faecalis* | N/A | **QNSPNIFGQWM*** |
| *L. plantarum* | N/A | CVGIW* |
| *L. innocua* | N/A | SKACFMFV* |
| *L. monocytogenes* | N/A | **ACFMFV** |
| *L. welshimeri* | N/A | SKACFMFV |

*AIP sequences that have been previously identified, **bold** sequences are AIP sequences confirmed in this study, yellow highlighted sequences are AIP sequences identified in this study. All other AIP sequences are predicted AIP sequences based on gene transcription. Red residues are the identified/predicted residue that forms the thiolactone or lactone ring with the c-terminus [39].

Recently, a new generation of high resolving power hybrid mass spectrometers has been developed that employs a combination of quadrupole and Orbitrap mass analyzers. Relying on the exceptional sensitivity and mass accuracy of this new mass spectrometer design, in combination with the outstanding chromatographic resolution

achievable with ultra-high performance liquid-chromatography (UHPLC), we developed a method to directly identify, detect, and quantify AIP in the crude growth media of multiple Gram-positive bacteria. Using our newly developed method, we compared the potency of known quorum sensing inhibitor ambuic acid across multiple strains of Gram-positive bacteria. This study is the first to demonstrate the application of a mass spectrometry-based approach for determining $IC_{50}$ values for AIP inhibition.

## 2.2 Materials and Methods

### 2.2.1 Instrumentation

Optical density readings were performed using a Synergy H1 Mutli-Mode Reader (Biotek Instruments, Inc., Winooski, VT). Unless otherwise stated, liquid chromatography-mass spectrometry (LC-MS) analyses were performed using an Aquity ultra-high performance liquid chromatography (UPLC) system (Waters Corporation, Milford, MA) coupled to a Q Exactive Plus Hybrid Quadrupole-Orbitrap mass spectrometer (Thermo Fisher Scientific, Waltham, MA). Unless otherwise stated, all solvents used for chemical analyses were purchased from Thermo Fisher Scientific (Waltham, MA)

### 2.2.2 Bacterial Strains, Media and Growth Conditions

Bacterial strains used in this study are listed in Table 2. All strains were provided by the Horswill lab at University of Iowa, Iowa City, Iowa. Strains AH335 and LS1 were maintained in Brain Heart Infusion broth (Teknova, Hollister, CA). All other strains were maintained in Tryptic Soy broth (Sigma Aldrich, St. Louis, MO).

**Table 2. Bacteria Strains**

| Species | Strain Number | *Description* |
|---|---|---|
| *Enterococcus faecalis* | AH3335 | ATCC Strain 47077/ OG1RF |
| *Listeria monocytogenes* | LS1 | EGDe serotype 1/2a [47] |
| *Staphylococcus aureus* | AH1263 | WT USA300 LAC MRSA (*agr* type I) |
| | AH2623 | USA100 (*agr* type II) |
| | AH759 | UAMS-1 Clinical isolate (*agr* III) [48] |
| *Staphylococcus epidermidis* | 4804 | Clinical isolate (*agr t*ype I) [44] |
| | 5183 | Clinical isolate (*agr* type II) [44] |
| | 5794 | Clinical isolate (*agr t*ype III) [44] |
| *Staphylococcus lugdunensis* | AH2160 | N920 143 (*agr* type I) |
| *Staphylococcu saprophyticus* | AH2776 | ATCC 15305 |

### 2.2.3 Identification and Detection of Auto-Inducing Peptides

Single isolated colonies of each strain were grown overnight at 37 °C. Overnight cultures were then diluted 1:200 (bacterial culture:broth) and shaken for at least 16 hr at 200 rpm and 37 °C. Cells were pelleted by centrifugation at 6,000 × g for 5 min and removed by 0.22-μm filtration. AIP was detected directly from spent media filtrate using LC-MS.

To conduct LC-MS analyses, a 7 μL injection of each sample was eluted from the column (Acquity UPLC BEH C18 1.7μm, 2.1 × 50 mm, Waters Corp.) at a flow rate of 0.3 mL/min using the following binary gradient with solvent A consisting of water (Optima LC/MS grade) with 0.1% formic acid additive and solvent B consisting of acetonitrile (Optima LC/MS grade) with 0.1% formic acid additive. The gradient initiated at 90:10 (A:B) and increased linearly from 0.0-8.0 min to 40:60 (A:B), followed by an isocratic hold at 40:60 (A:B) from 8.0-8.5 min, gradient returned to starting conditions of 90:10 (A:B) from 8.5-9.0 min, and was held at this composition from 9.0-10 min.

Mass spectra were collected using two scan events. The first scan event was a positive mode full scan with a mass range from 300 – 2000 and a resolution of 70,000. The second scan event was positive mode selected ion monitoring for the calculated mass of the predicted/identified AIP with an isolation window of 1 amu. Predicted *m/z* values were determined by using the known AgrD sequence as a guide. Starting with an initial 8 residue sequence, amino acid residues were added and subtracted from the N-terminus. The mass spectrometer was operated using a heated electrospray ionization source with the following setting: capillary temperature set at 300°C, S-Lens RF level set at 80, spray voltage set at 4.0 kV, sheath gas flow set at 50 (arbitrary units), and auxiliary gas flow set at 15.

2.2.3.1 Confirmation of *Listeria monocytogenes* AIP

Confirmation of correct AIP identification was achieved through MS-MS analysis. The calculated AIP *m/z* value, 699.29985, was selected as precursor ion and subjected to high-energy collision dissociation (HCD) at normalized collision energy of 23. Resulting spectra were compared to predicted fragmentation pattern of AIP ion. Fragmentation prediction was performed on ACD Labs fragment predictor.

2.2.3.2 Confirmation of *Staphylococcus saprophyticus* AIP

Confirmation of correct AIP identification was achieved through MS-MS analysis using a Thermo Fisher LTQ Orbitrap XL Hybrid Ion Trap-Orbitrap mass spectrometer coupled to an Aquity UPLC system using the same instrument settings listed above. Calculated AIP *m/z* value, 896.39764, was selected as precursor ions and subjected to

collision induced dissociation (CID) at normalized collision energy of 35. Resulting spectra were compared to predicted fragmentation pattern of AIP ion.

### 2.2.4 Ambuic Acid Inhibition Assays

Assays to evaluate inhibition by ambuic acid were performed in a 96-well plate format. Overnight cultures were diluted 1:200 (culture:broth) and shaken (200 rpm) at 37 °C for two hours. An aliquot of this culture (200 μL) was then combined with 45 μL broth and 5 μL dimethyl sulfoxide (DMSO) containing ambuic acid (Adipogen International, San diego, CA) in concentrations ranging from 20 μM to 10 mM prepared in two-fold serial dilutions. Final ambuic acid concentration in the assay wells ranged from 390 nM to 200 μM. Plates were shaken at 1000 rpm at 37 °C using a Stuart S1505 microtitre plate shaker (Bibby Scientific Limited, Staffordshire, U.K.). Cell growth was monitored by measuring absorbance at 600 nm at one hour intervals. Cells were grown to the end of the log-phase and were removed via vacuum filtration. Filtrate was analyzed using LC-MS method described above. Selected ion chromatograms for the identified AIP *m/z* values were plotted and peak area values were used for relative AIP concentration comparison. $IC_{50}$ values were determined from a four parameter logistic function using Sigma plot 12.5.

## 2.3 Results

### 2.3.1 Identification of AIPs

Using the hybrid quadrupole-Orbitrap mass spectrometer in combination with published gene sequence data, it was possible to identify AIPs directly from spent media of bacterial cultures. The method was applied to detect and sequence AIPs from

*Staphylococcus aureus*, *Staphylococcus epidermidis*, *Staphylococcus lugdunensis*, and *Enterococcus faecalis*. Results agreed with reported data for *S. aureus* [39, 41, 49], *S. epidermidis*[44], *S. lugdunensis* [49], and *E. faecalis* [42], strains for which AIPs have previously been reported, and were also used to identify unknown AIPs in *Listeria monocytogenes* and *Staphylococcus saphrophyticus*.

Identification of the *L. monocytogenes* AIP was enabled by detection of an ion with *m/z* of 699.29910 in spent media. This value corresponded to the cyclic hexapeptide Ala-c(Cys-Phe-Met-Phe-Val) containing a thiolactone ring linked between the sulfhydryl group of the cysteine and the α-carboxyl group of the C-terminal valine (calc. *m/z* 699.29985, mass error 1.5 ppm). For *S. saphrophyticus*, an ion with *m/z* 896.3971 was identified. This value corresponded to the cyclic octapeptide Ile-Asn-Pro-c(Cys-Phe-Gly-Tyr-Thr) containing a thiolactone ring linked between the sulfhydryl group of the cysteine and the α-carboxyl group of the C-terminal threonine (calc. *m/z* 896.39764, mass error of 2.6 ppm). Identified ions were subjected to fragmentation and the resulting product ions were in agreement with the predicted fragmentation patterns for these peptides (Figures 5 and 6).

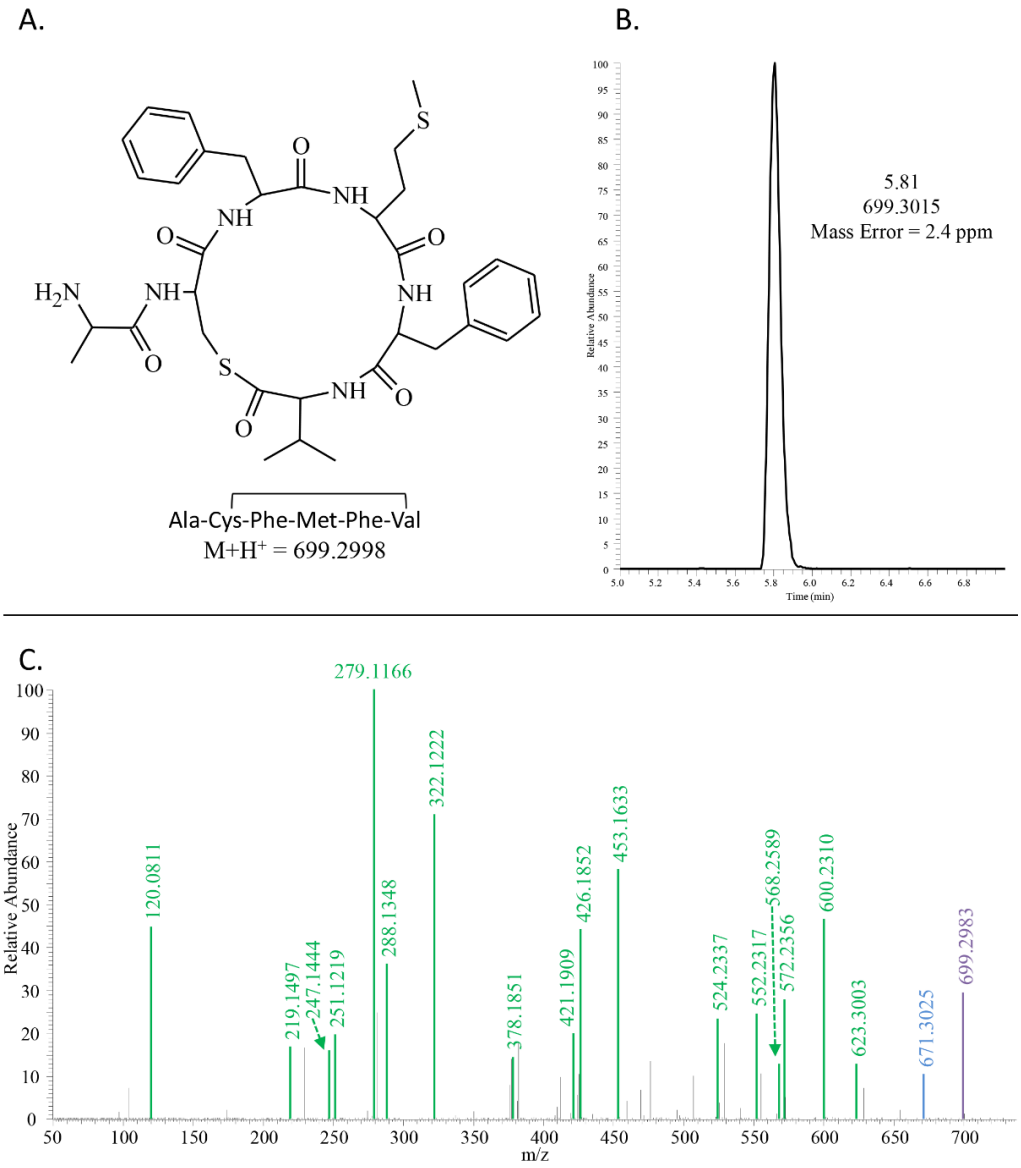


**Figure 5. Identification of *Listeria monocytogenes* AIP.**

Structure, sequence and accurate mass of the $[M+H]^+$ ion for the identified *L. monocytogenes* AIP are shown in panel A. Selected-ion chromatogram for *m/z* 699.2998 (B) was used to detect AIP, and higher-energy collision dissociation (HCD) MS-MS fragmentation pattern of the ion with retention time of 5.81 min and *m/z* of 699.3015 (C) was used to confirm correct identification. In panel C, the purple peak is unfragmented precursor ion, the blue peak is representative a water loss, and the green peaks match within 3 ppm mass error of predicted fragment ions.

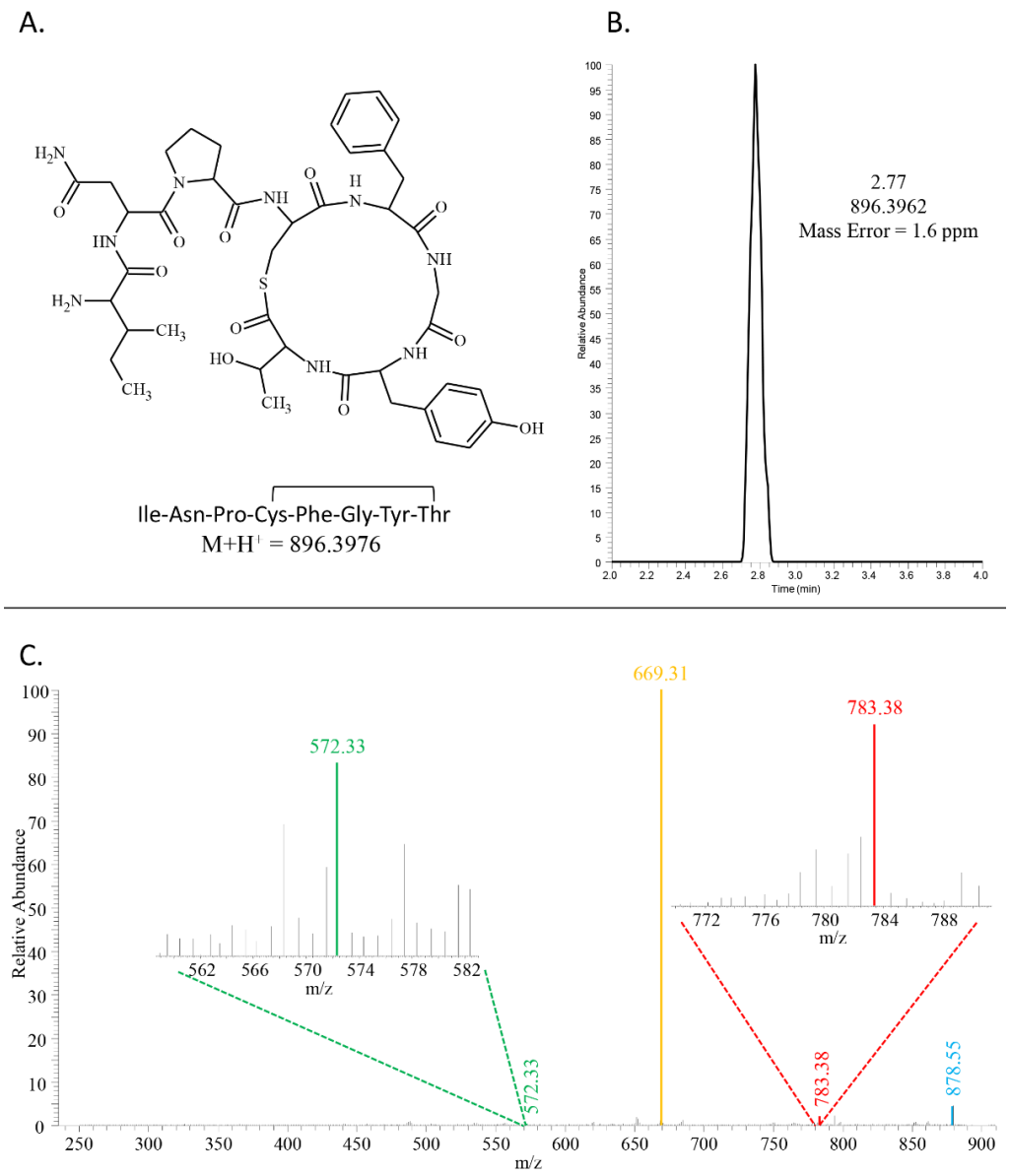


**Figure 6. Identification of *Staphylococcus saphrophyticus* AIP.**

Structure, sequence and accurate mass $[M+H]^+$ for the identified *S. saphrophyrius* AIP are shown in panel A. Selected-ion chromatogram for *m/z* 896.3976 (panel B) was used to detect AIP, and collision-induced dissociation (CID) MS-MS fragmentation pattern (C) was used to confirm correct identification. Blue peak is representative a water loss, red peak matches the expected *m/z* for the $y_7$ fragment, yellow peak matches the expected *m/z* for the $y_6$ fragment, and the green peak matches the expected *m/z* for the $y_6$ fragment.

### 2.3.2 Quantification of AIP

Once the identification of all AIPs was confirmed, the peak area for the relevant AIP ion could be monitored to compare AIP production under different treatment conditions. Known *agr* system inhibitors of *S. aureus* were tested against a clinical isolate of methicillin-resistant *Staphylococcus aureus* (USA300 LAC strain, AH1263) strain (Figure 7), and the resulting chromatographic peak corresponding to AIP I was significantly ($p < 0.001$) reduced compared to the untreated control, indicating AIP inhibition could be directly monitored via LC-MS. Ambuic acid, a known AgrB inhibitor [50] discussed in more detail in Section 2.3.3, was tested in varying concentrations to determine if the described method could detect the decreasing concentration of AIP in a dose dependent manner. The resulting selected-ion chromatograms (Figure 8) represent AIP concentration decreasing as the concentration of the inhibitor increases. The peak area of the selected-ion chromatogram for *m/z* 961.3799 (AIP-I) was plotted against the concentration of ambuic acid, resulting in a dose-response curve from which an $IC_{50}$ value could be determined (Figure 9).

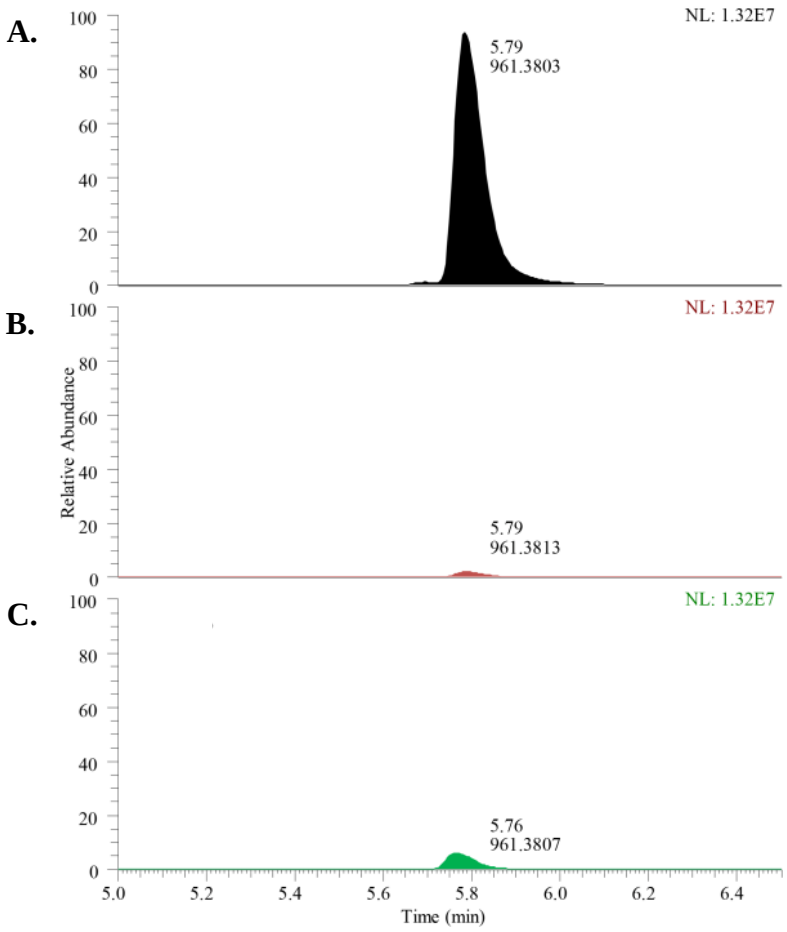


**Figure 7. Inhibition of *S. aureus Agr* System.**

Selected-ion chromatograms (*m/z* 961.3788) obtained by LC-MS analysis of the spent broth from a culture of the clinical MRSA USA300 LAC strain (AH1263). The chromatogram for the strain grown without the *agr* system inhibitor (A) is compared to chromatograms of the strain grown with 50 μM of an AgrB inhbitor (ambuic acid) (B), and with 4.5 μM of an AgrC inhibitor (AIP II) (C).

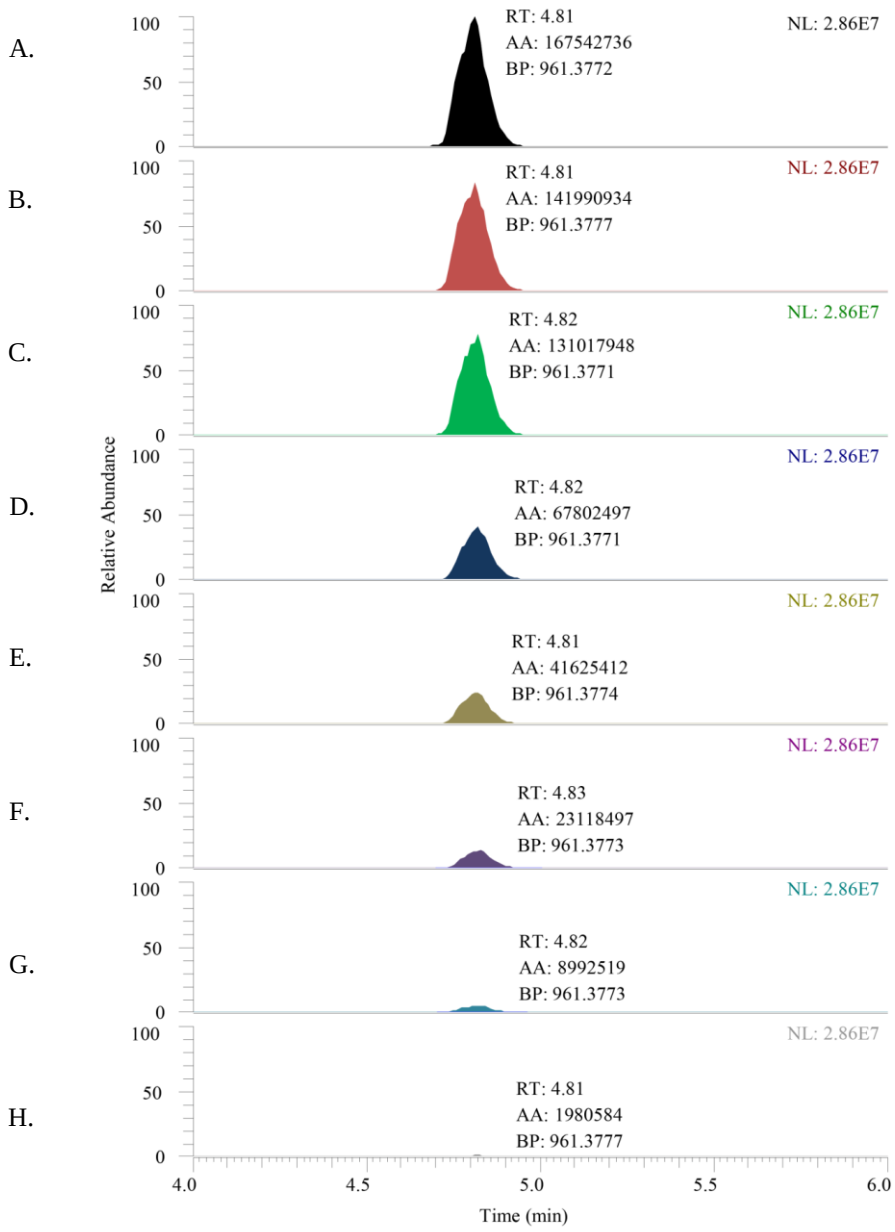


**Figure 8. Inhibition of AIP Production by MRSA (AH1263) with Ambuic Acid**

Selected-ion chromatograms (*m/z* 961.3799) showing a decreasing peak area for AIP in response to an increasing concentration of ambuic acid in the growth media. Concentration of ambuic acid from A to H: 0 µM, 0.39 µM, 0.78 µM, 1.6 µM, 3.1 µM, 6.3 µM, 13 µM, 25 µM. RT indicates the retention time, AA indicated the peak area and BP indicates the observed *m/z* value for the chromatographic peak.

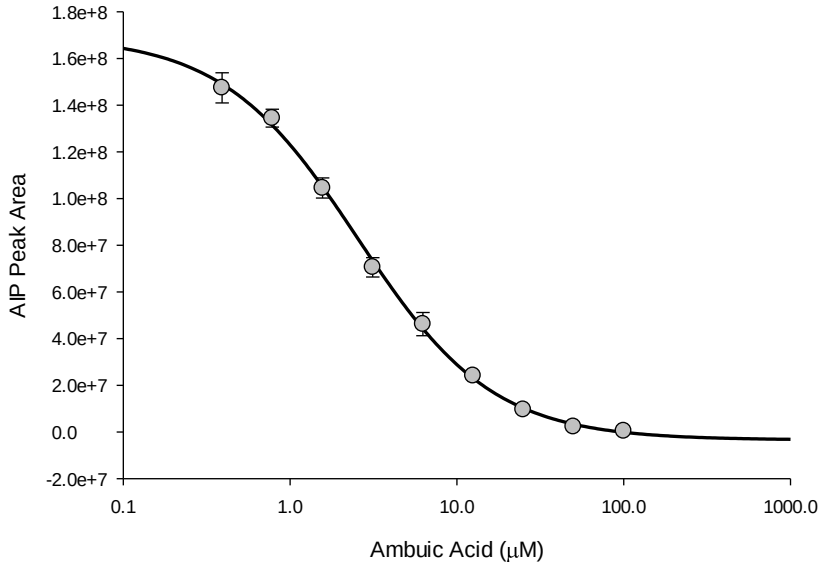


**Figure 9. Dose-Response Curve for Ambuic Acid**

Dose-response curve for peak area of AIP as a function of ambuic acid concentration. Curve fitting was accomplished using a four parameter logistic equation in Sigma Plot 12.

### 2.3.3 Broad Applicability of Ambuic Acid as a Quorum Sensing Inhibitor

A number of *S. aureus agr* system inhibitors have previously been identified in literature [33-36, 40, 50-52], including the small molecule fungal metabolite ambuic acid. Nakayama *et. al.* suggested that ambuic acid should be broadly applicable against multiple strains of Gram-positive bacteria, and provided some data indicating inhibition of AIP production by ambuic acid against *Enterococcus faecalis*, *Staphylococcus aureus* and *Listeria innocua*. Using the method developed herein, we expanded these studies to compare $IC_{50}$ values for ambuic acid against multiple bacterial strains, four species of Staphylococci (*S. aureus*, *S. epidermidis*, *S. lugdunensis*, and *S. saprophyticus*), *Listeria monocytogenes* and *E. faecalis*. Inhibition against three *agr* types of *S. aureus* (type I-III)

and three *agr* types of *S. epidermidis* (type I-III) was also evaluated. Table 3 shows the $IC_{50}$ values determined for the various bacterial strains. The $IC_{50}$ for AIP inhibition by ambuic acid was less than 25 µM in 8 of the 11 strains tested in this study, with the most potent inhibition observed against *E. faecalis* ($IC_{50}$ 1.8 ± 0.7 µM). Surprisingly, very little inhibition was observed for *S. lugdunensis agr* type I and *S. epidermidis agr* types II and III ($IC_{50}$ values greater than 200 µM).

**Table 3. $IC_{50}$ Values for Ambuic Acid Inhibition of AIP Biosynthesis**

| Strain ID | Species | *Agr* Type | $IC_{50}$ (µM) | AIP Sequence |
|---|---|---|---|---|
| AH3335 | *E. faecalis* | *N/A* | 1.8 ± 0.7 | QNSPNIFGQWM[a] |
| LS1 | *L. monocytogenes* | *N/A* | 8.7 ± 0.2 | ACFMFV[a] |
| AH1263 | *S.aureus* | *Type I* | 2.5 ± 0.1 | YSTCDFIM[a] |
| AH2623 | *S.aureus* | *Type II* | 23.6 ± 3.5 | GVNACSSLF[a] |
| AH759 | *S. aureus* | *Type III* | 10.1 ± 0.3 | INCDFLL[a] |
| 4804 | *S. epidermidis* | *Type I* | 15.1 ± 2.8 | DSVCASYF[a] |
| 5183 | *S. epidermidis* | *Type II* | >200 | NASKYNPCSNYL[a] |
| 5794 | *S. epidermidis* | *Type III* | >200 | NAAKYNPCASYL[a] |
| AH2160 | *S. lugdunensis* | *Type I* | >200 | DICNAYF[a] |
| AH2776 | *S. saprophyticus* | *N/A* | 2.6 ± 1.5 | INPCFGYT[a] |

[a] Residues indicated with red form the thiolactone or lactone ring with the c-terminus.

### 2.3.4 Growth Effects

AIP is produced in a density dependent manner, meaning higher cell density yields higher AIP concentration. For this reason, any growth inhibition can easily be

misinterpreted as *agr* system inhibition. In order to rule out this confounding factor, cell growth was monitored by collecting $OD_{600}$ readings at 1 hr intervals leading up to the final AIP measurement for each experiment. Inspection of the resulting growth curves demonstrated no significant growth inhibition by ambuic acid at concentrations below 200 µM for any of the strains tested in this study, as demonstrated by the representative growth curve in Figure 10. Growth inhibition was observed at concentrations above 200 µM, so AIP inhibition was not evaluated above this concentration.

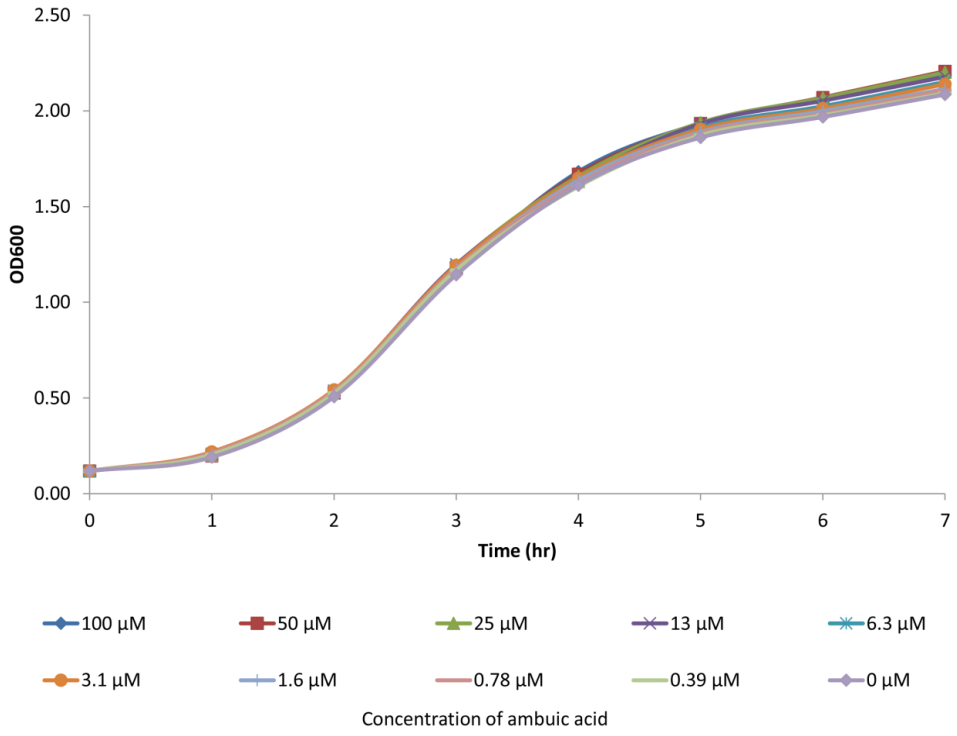


**Figure 10. Growth Curve for *S. aureus Agr* Type I with Ambuic Acid**

Evaluation of growth effect for the varying concentrations of ambuic acid was accomplished by the comparison of growth curves. Ambuic acid was tested at concentrations ranging from 0 µM to 100 µM over a 7 hr time period. No growth effects were observed for these concentrations of ambuic acid.

## 2.4 Discussion

The present study utilizes the ability to detect and quantify AIP in the complex growth media of a bacteria culture to provide insight into *agr* system activity. Knowing the correct AIP structure for a species of bacteria is also a valuable tool for studying a wide range of cellular functions. This study focused primarily on the link between the *agr* system and virulence, however the agr system has also been linked to biofilm formation, an important mechanism in antibiotic resistance [39]. Current methods for monitoring *agr* system activity rely on either colorimetric responses [51], which can be difficult to accurately quantify, or luminescence/fluorescent methods [33, 50, 53], which require genetically modifying the organism of interest and are potentially susceptible to interference in complex matrixes. The method developed herein requires only knowledge of the AIP structure, and allows for the direct monitoring of the *agr* system of the organism of interest, making it applicable to clinically relevant strains of bacteria. Using the developed method, an $IC_{50}$ value for ambuic acid was determined against a variety of Gram-positive bacteria. While ambuic acid has been previously identified as an *agr* system inhibitor, no $IC_{50}$ values for this compound have been reported.

It is interesting to note that two of the three strains that showed little response to treatment with ambuic acid were strains of *S. epidermidis*, a human commensal of the skin and mucosal surfaces. *S. epidermidis* may help inhibit the colonization of more pathogenic bacteria, such as *S. aureus* [54-56]. Therefore, it might be advantageous to inhibit the *agr* system of more pathogenic bacteria while leaving some *S. epidermidis* strains functioning normally. The observation that ambuic acid doesn't inhibit two of the

three *agr* types of *S. epidermidis* may offer further insight into ambuic acid's mode of action, and could be the topic of future studies.

## 2.5 Conclusion

Anti-virulence has proven to be a promising method for combating bacterial infections in animal models [33, 35], and the *agr* system is an ideal target for inhibiting virulence in a wide variety of Gram-positive bacteria. The presented study utilized the technological advances in mass spectrometry as a basis for broadly applicable method for monitoring *agr* system activity. We presented the structure of two new AIPs, *S. saprophyticus* and *L. monocytogenes*, and used our newly developed method to measure the $IC_{50}$ values of ambuic acid inhibition against a variety for Gram-positive bacteria. Our results demonstrate the potential usefulness of ambuic acid as a broad spectrum *agr* system inhibitor.

# CHAPTER III

# DEVELOPMENT OF A BIOASSAY TARGETING AIP BIOSYNTHESIS

## 3.1 Introduction

The past four decades of drug discovery have been marked by a drastic decline in antibiotic discovery, with only 2 new classes of antibiotics discovered since 1968 [4]. Unfortunately, this time period also saw a rapid increasing presence of antibiotic resistant bacteria [1], leading some healthcare professionals to believe we are rapidly approaching a "post-antibiotic" era. While the discovery of new antibiotics may aid in the continual fight against bacterial infections, it is imperative to identify new therapeutics that function through novel mechanisms of action.

Quorum sensing is used by bacteria to regulate numerous cellular functions. In Gram-positive bacteria, the quorum sensing *agr* system has been linked to the production of virulence factors [37, 39, 40, 44, 57]. This makes the *agr* system an ideal target for therapeutics capable of combating bacterial infections. Previous research has proven the viability of targeting the *agr* system in *Staphylococcus aureus* to fight off these infections [33-36, 39, 40, 51, 57, 58], and the common presence of the *agr* system throughout a variety of Gram-positive bacteria [39] shows the possibility of the *agr* system to serve as a broad-spectrum target.

The *agr* system is comprised of two primary regions, a two-component regulatory cascade and a signal biosynthesis region. The two-component regulatory cascade consists of AgrC, an integral membrane sensor, and AgrA, a response regulator. The signal biosynthesis region contains AgrB, a membrane-bound peptidase, and AgrD, a propeptide to the *agr* system activator AIP [36, 39] (Figure 4). Currently, the majority of published *agr* system inhibitors target the regulatory cascade region of the *agr* system [34]. While most of these studies focus on competitively inhibiting AgrC [51, 59, 60], some have identified molecules capable of inhibiting AgrA [33, 61, 62]. Unfortunately, AgrC may not be the ideal target for a broad-spectrum quorum sensing inhibitor due to the high variability in its sequence throughout different bacterial species [39] and its propensity to be hypermutable [34, 63]. AgrB, however, is relatively conserved throughout most species of Gram-positive bacteria [39] and spans across the cytoplasmic membrane. Therefore, the AIP biosynthesis region may be an ideal target for broad-spectrum quorum sensing inhibition.

Nakayama *et. al.* identified the small molecule fungal metabolite ambuic acid as an inhibitor of the *fsr* system in *Enterococcus faecalis* an analogous *agr* system. Their study suggested inhibition of FsrB (AgrB analog) as the mode of action for this compound. This conclusion was based on their observation that, when treated with ambuic acid, the *Fsr* system was inactive but could be reactivated with the addition of synthetic GBAP (an AIP analog) [50]. Additional studies performed in our laboratory (Chapter I) showed the potential of ambuic acid to act as a broad-spectrum *agr* system

inhibitor, confirming that the AIP biosynthesis region of the *agr* system is viable target for broad-spectrum quorum sensing inhibition.

Ambuic Acid is currently the only known AIP biosynthesis inhibitor. The purpose of this study was to develop a novel biological assay to specifically screen for new AIP biosynthesis inhibitors. The Horswill lab at the University of Iowa (Iowa City, IA), engineered a strain of *S. aureus* to contain only the genes that encode for AgrB and AgrD. The resulting strain continuously produced AIP unless inhibited by a compound specifically targeting AIP biosynthesis. By combining the previously established method for efficiently quantifying AIP production (Chapter I) with this newly developed strain of *S. aureus,* complex mixtures and pure compounds could be rapidly evaluated for their ability to inhibit AIP biosynthesis. This method has allowed us to efficiently screen over 500 natural product compounds, as well as confirm ambuic acid's mode of action.

## 3.2 Materials and Methods

### 3.2.1 Instrumentation

Optical density readings were performed using a Synergy H1 Mutli-Mode Reader (Biotek Instruments, Inc., Winooski, VT). Liquid chromatography-mass spectrometry (LC-MS) was performed using an Aquity ultra-high performance liquid chromatography (UPLC) system (Waters Corporation, Milford, MA) coupled to a Q Exactive Plus Hybrid Quadrupole-Orbitrap mass spectrometer (Thermo Fisher Scientific, Waltham, MA). Unless otherwise stated, all solvents used for chemical analyses were purchased from Thermo Fisher Scientific (Waltham, MA)

### 3.2.2 Bacterial Strains, Media and Growth Conditions

The Horswill lab at University of Iowa, Iowa City, Iowa, provided all bacteria strains used in this study (Table 4).

**Table 4. Bacteria Strains**

| Strain | Description | Reference |
|---|---|---|
| AH1263 | Erm-sensitive CA-MRSA USA300-0114 | [64] |
| AH1292 | AH1263 Δ*agr*::TetM | [65] |
| AH2989 | AIP Constitutively Producing Strain | This work |

### 3.2.3 Engineering of AIP Constitutively Producing Strain (AH2989)

Strain AH2989 was constructed in a series of steps. Initially, the sarA P1 promoter was amplified by PCR from the AH1263 genome using oligonucleotides ARH120 (5'-GTTGTTAAGCTTCTGATATTTTTGACTAAACCAAATGC-3') and CLM607 (5' -CACCACTCTCCTCACTGTCTCTAGAGATGCATCTTGCTCGATACA TTTG-3'). The PCR product was purified, digested with HindIII and XbaI, and cloned into plasmid pLL29 [66]. Next, the agrBD genes from AH1263 (agr type I) were amplified by PCR using CLM608 (5'-TCTAGAGACAGTGAGGAGAGTGGTGTAAA ATTG -3') and CLM606 (5'-GTTGTTGAATTCCTATTTAAATTATTCGTGTAATTG TG-3'). The PCR product was purified, digested with XbaI and EcoRI, and cloned into pLL29 downstream of the sarA P1 promoter. Plasmid pLL29 with the sarA P1 promoter driving agrBD was integrated into RN4220 using the protocol previously described [66]. The integrated construct was crossed by 80α phage transduction into AH1263 by selecting for tetracycline resistance. The Δagr::TetM construct was subsequently crossed

from AH1292 into this strain by selecting for minocycline resistance, which is conferred by the TetM marker**.**

### 3.2.4 Pure Compounds for Screening

A natural products library containing 144 compounds was purchased from Selleckchem (Houston, TX). The Oberlies lab at the University of North Carolina Greensboro provided an additional 426 natural product compounds. The positive control ambuic acid was purchased from Adipogen International, San diego, CA.

### 3.2.5 Screening for AIP Biosynthesis Inhibitors

Bacteria cultures were prepared as previous described in Section 2.2.3.

Samples dissolved in 1:1 dioxane:methanol were aliquoted into a 96-well plate with 1 mL wells. 10 µL of sterilized glycerol was added to each well, and the 96-well plate was vacuum concentrated for 1.5 hr to facilitate the removal of dioxane:methanol. Dimethyl sulfoxide was added to each well until final sample concentration was 1.25 mM per well. Sample (5 µL) was combined with 45 µL of TSB and 200 µL of 2 hr bacteria culture in a 200 µL clear bottom 96-well plate, resulting in a final sample concentration of 25 µM per well. For the first stage of screening samples were tested in a single well. Samples moved forward to the second stage of screening were tested in triplicate. A vehicle control was prepared by subjecting a blank aliquote of 1:1 dioxane:methanol to all previously described steps. Ambuic acid was used as a positive control, and both negative and positive controls were analyzed in triplicate (biological replicates) with every assay.

The plate was shaken at 1000 rpm at 37 °C using a Stuart S1505 microtitre plate shaker (Bibby Scientific Limited, Staffordshire, U.K.) and cell growth was monitored in one-hour intervals using an optical density of 600 nm. Cells were grown to the end of the log-phase, approximately 5 hr, and were removed via vacuum filtration. The filtrate was analyzed using LC-MS.

For the LC-MS analysis, a 7 µL injection of each sample was eluted from the column (Acquity UPLC BEH C18 1.7µm, 2.1 × 50 mm, Waters Corp.) at a flow rate of 0.3 mL/min using the following binary gradient with solvent A consisting of water (Optima LC/MS grade) with 0.1% formic acid additive and solvent B consisting of acetonitrile (Optima LC/MS grade) with 0.1% formic acid additive. The gradient initiated at 75:25 (A:B) and increased linearly from 0.0-3.5 min to 50:50 (A:B), followed by a linear increase to 0:100 (A:B) from 3.5-4.0 min, gradient returned to starting conditions of 75:25 (A:B) from 4.0-4.5 min, and was held at this composition from 4.5-5.0 min.

The mass spectra were collected using a positive mode selected ion monitoring scan event. An *m/z* value of 961.3799 was selectively monitored with a 1 amu isolation window. This value corresponds with the calculated *m/z* value for the AIP produced. The mass spectrometer was operated using the same parameters described in Section 2.2.3

### 3.2.6 Quantification of AIP

Using Thermo Fisher Scientific's Xcalibur software the selected ion chromatogram for *m/z* 961.3799 plotted and the corresponding peak area was used for relative AIP quantity determination. An automatic processing method was designed to

facilitate rapid and consistent peak integration. The automatic processing method utilized the base peak chromatogram trace with a selected *m/z* value of 961.3799 and a mass tolerance of 5 ppm. The Genesis peak detection algorithm with 7 smoothing points and a 0.5 signal to noise threshold was used for peak integration. A 30 sec retention time window was set at 2.35 min.

## 3.3 Results

### 3.3.1 Development of Targeted Bioassay

Inhibiting the quorum sensing *agr* system has proven to be viable mechanism for combating Gram-positive pathogens [33-35]. Specifically targeting AgrB has the implication for development of a broad-spectrum quorum sensing inhibitor. Until now, no efficient method has been developed to efficiently screen for AgrB inhibitors. In the present study, we use the combination of a uniquely engineered strain of *S. aureus* (AH2989) and an efficient mass spectrometry-based method for AIP detection to create a novel biological assay specifically designed to facilitate the discovery of new AIP biosynthesis inhibitors (Figure 11).

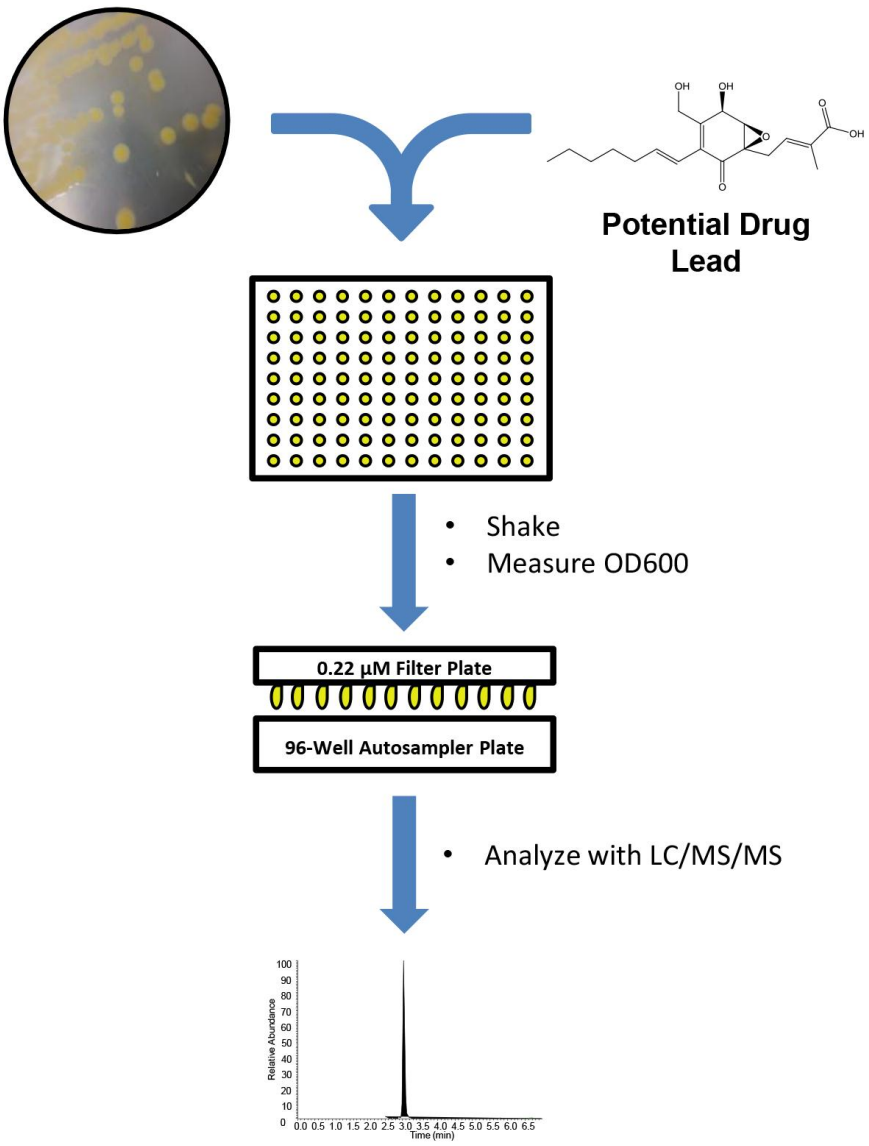


**Figure 11. Bioassay Workflow**

The workflow shown here allows for the rapid screening of multiple drug leads at one time. A single colony bacterial culture is combined with 90 potential drug leads in one 96-well plate. Positive and negative controls are analyzed in triplicate throughout the plate. The OD600 is measured every hr to evaluate cell growth. Once the bacterial growth reaches the end of the log-phase, approximately 6 hr, cells are removed via vacuum filtration, and filtrate is analyzed using LC-MS.

### 3.3.2 Confirmation of Ambuic Acid's Mode of Action

A comparison between the observed *agr* system inhibition between the AIP constitutively producing strain (AH2989) and the USA300 strain (AH1263) was performed to ensure that AIP biosynthesis inhibitors would selectively inhibit the AIP constitutively producing strain (AH2989). Using the workflow out lined in Figure 11, ambuic acid, a compound previously proposed to act as an AIP biosynthesis inhibitor [50], and AIP II, the signaling molecule produced by *S. aureus agr* type II with the amino acid sequence Gly-Val-Asn-Ala-c(Cys-Ser-Ser-Leu-Phe) and known to inhibit AgrC [39], were tested against both strains. Confirmation of ambuic acid's mode of action could also be achieved through this experiment.

Ambuic acid inhibited the production of AIP by the AIP constitutively producing strain (AH2989), indicating it does inhibit AIP biosynthesis (Figure 12). Ambuic acid also inhibits AIP production in the USA300 strain (AH1263) (Figure 12). However, AIP II, a known AgrC inhibitor, inhibited AIPI production by the USA300 strain (AH1263), but not by the AIP constitutively producing strain (AH2989). The observation that the known AgrC inhibitor was unable to inhibit the production of AIP in the constitutively producing strain (AH2989) indicates our assay will only identify compounds capable of inhibiting the AIP biosynthesis region of the *agr* system and not those inhibiting the signaling cascade. An $IC_{50}$ value of 6.6 ± 1.1 μM was determined for ambuic acid against the AIP constitutively producing strain (AH2989).

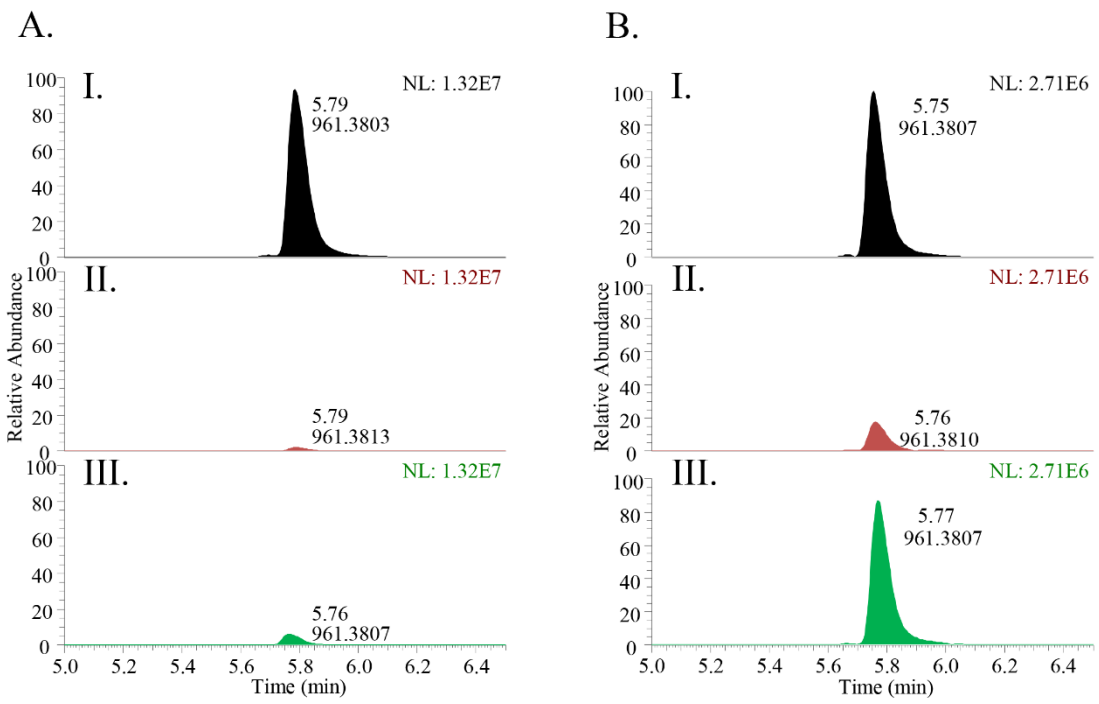


**Figure 12. Comparison of *Agr* System Inhibition**

Selected-ion chromatograms (*m/z* 961.3788) AI, AII, and AIII were all collected from the USA300 strain (AH1263), while BI, BII, and BIII were all collected from the AIP constitutively producing strain (AH2989). Chromatograms AI and BI were collected from uninhibited cultures, chromatograms AII and BII were collected from cultures grown with 50 µM ambuic acid, and chromatograms AIII and BIII were collected from cultures grown with 4.5 µM AIPII.

### 3.3.3 Growth Inhibition

As previously discussed in Section 2.3.4, growth inhibition can cause reduced AIP production that can be misconstrued as quorum sensing inhibition, and it was important to rule out this confounding factor. Growth was monitored by collecting $OD_{600}$ readings at 1 hr intervals leading up to the final AIP measurement for each experiment. Monitoring growth-curve data enabled viable leads as AgrB inhibitors to be distinguished from compounds that exerted their influence on AIP production due to growth effects.

Two types of growth effects can be observed, growth inhibition, which is indicated by a reduction in the endpoint $OD_{600}$ (Figure 13) and a growth delay (Figure 14), which reduces the $OD_{600}$ at various points throughout the growth curve but not at the final 24 hr time point. Without monitoring $OD_{600}$ at 1 hr intervals, a growth delay can easily be misconstrued as quorum sensing inhibition. For this study, only compounds showing < 25% growth inhibition were moved through the second stage of screening.

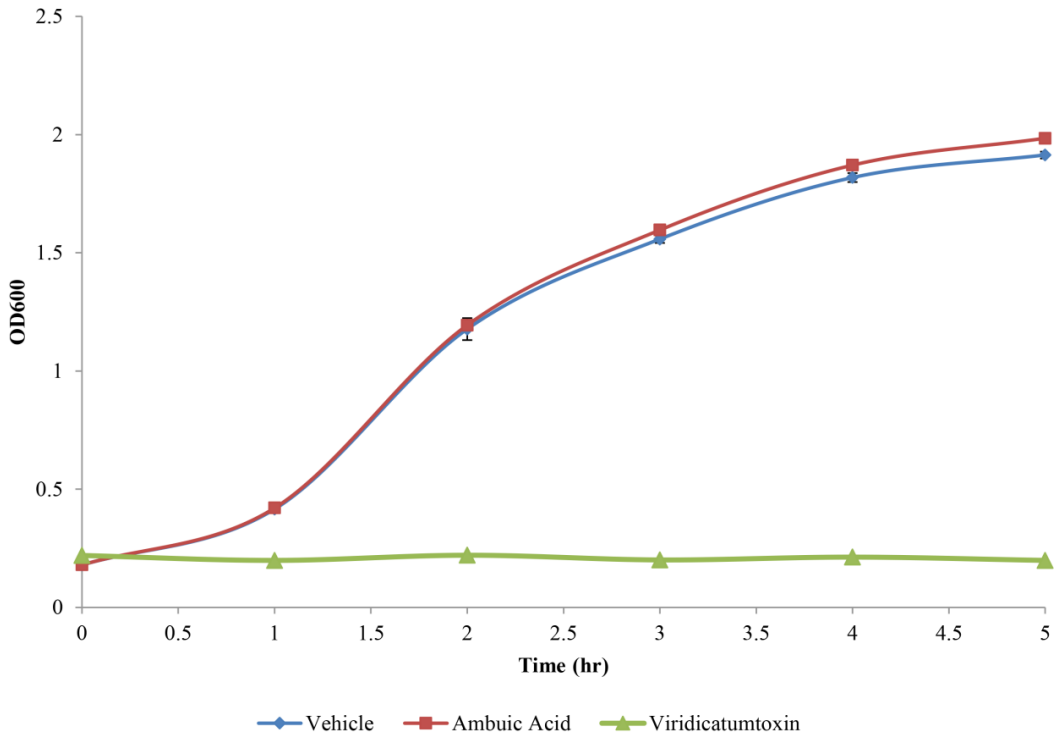


**Figure 13. Example of Growth Inhibition**

Viridicatumtoxin at 25 µM (green line) completely inhibited the growth of the AIP constitutively producing strain (AH2989), while ambuic acid at 100 µM (red line) and the vehicle control (blue line) showed no effect on growth.

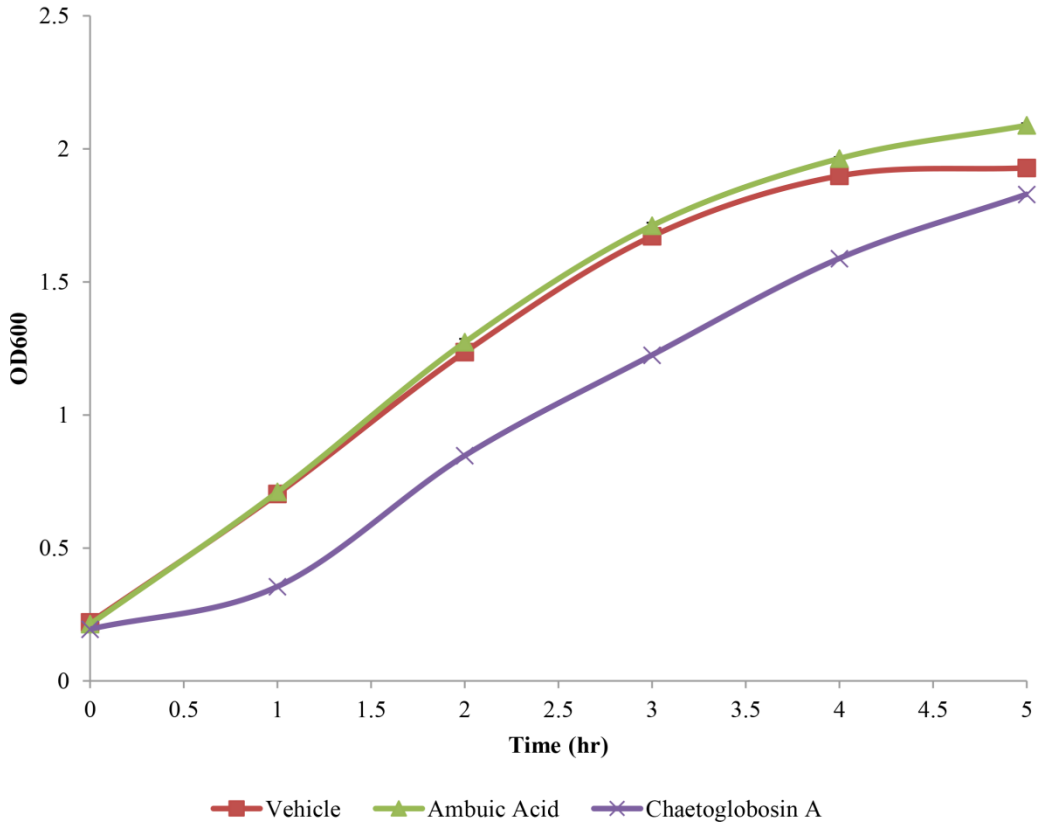


**Figure 14. Example of Growth Delay**

Chaetoglobsin A at 25 µM (green line) decreased the growth rate of the AIP constitutively producing strain (AH2989), while ambuic acid at 100 µM (red line) and the vehicle control (blue line) showed no effect on growth.

### 3.3.4 Natural Product Compound Screening

A number of natural product compounds (570) were subjected to the first stage of screening using our newly developed bioassay. The results of the assay are evaluated in two steps. The first step is an endpoint analysis, in which the endpoint AIP peak area and endpoint $OD_{600}$ for the samples are compared to the controls. Figure 15 shows a representative endpoint analysis in which the bars indicate AIP peak area and the line

indicated $OD_{600}$. Only compounds that showed greater than 40% AIP inhibition and less than 25% growth inhibition were moved to the second step evaluation. The first step evaluation reduced the sample size from 570 compounds down to 29.

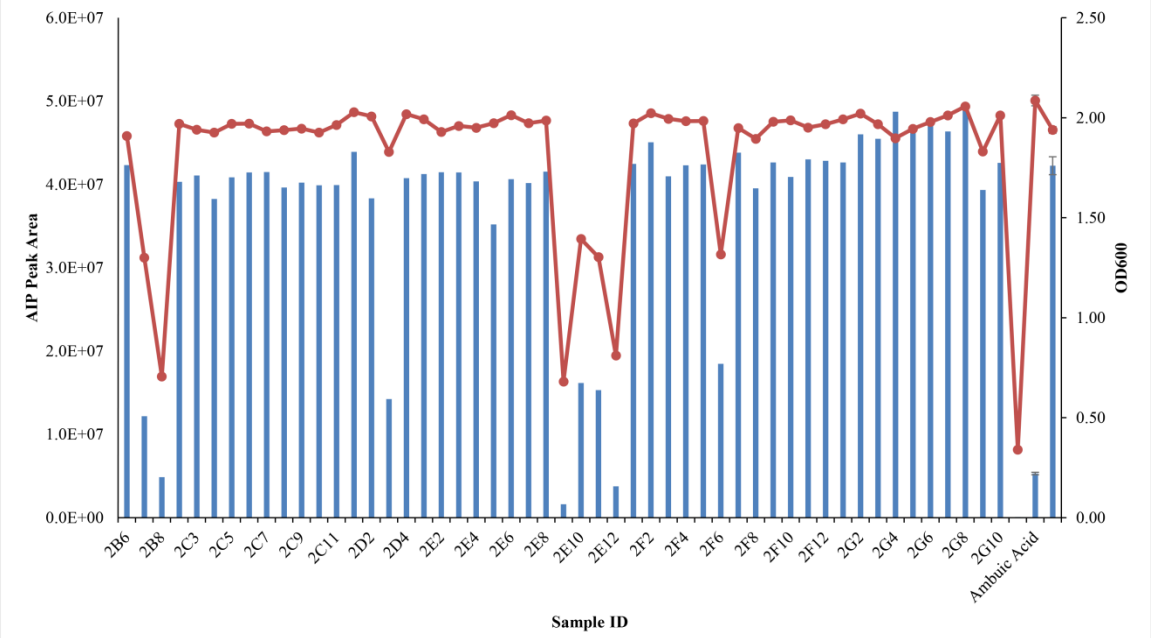


**Figure 15. Example of Endpoint Analysis**

Blue bars indicate AIP peak area and the red line indicates OD600 value (a measure of bacterial growth). The ambuic acid (positive control) represents desired results for a lead compound (drop in AIP peak area and no effect on growth). However, the majority of compounds tested (sample id), showed either no effect on either or had a decrease in both peak area and OD600. Compound 2D3, Chaetoglobsin A, appeared to be a potential lead and was subjected to growth curve analysis. Figure 14, shows the resulting growth curve from Chaetoglobsin A and indicated decrease in AIP peak was due to growth delay.

The remaining 29 sample results were subject to the second step of the evaluation in which the growth curves of the compounds were compared. Figure 16 shows a representative comparison of growth curves. The second step evaluation reduced the

sample size from 29 compounds down to four. The four potential leads were then subjected to the second stage of screening, in which all samples were evaluated in triplicate. Unfortunately, upon evaluation of the second stage assay results, it was concluded that all AIP inhibition was due to growth effects. An example of the second stage assay results can be found in Figure 17.

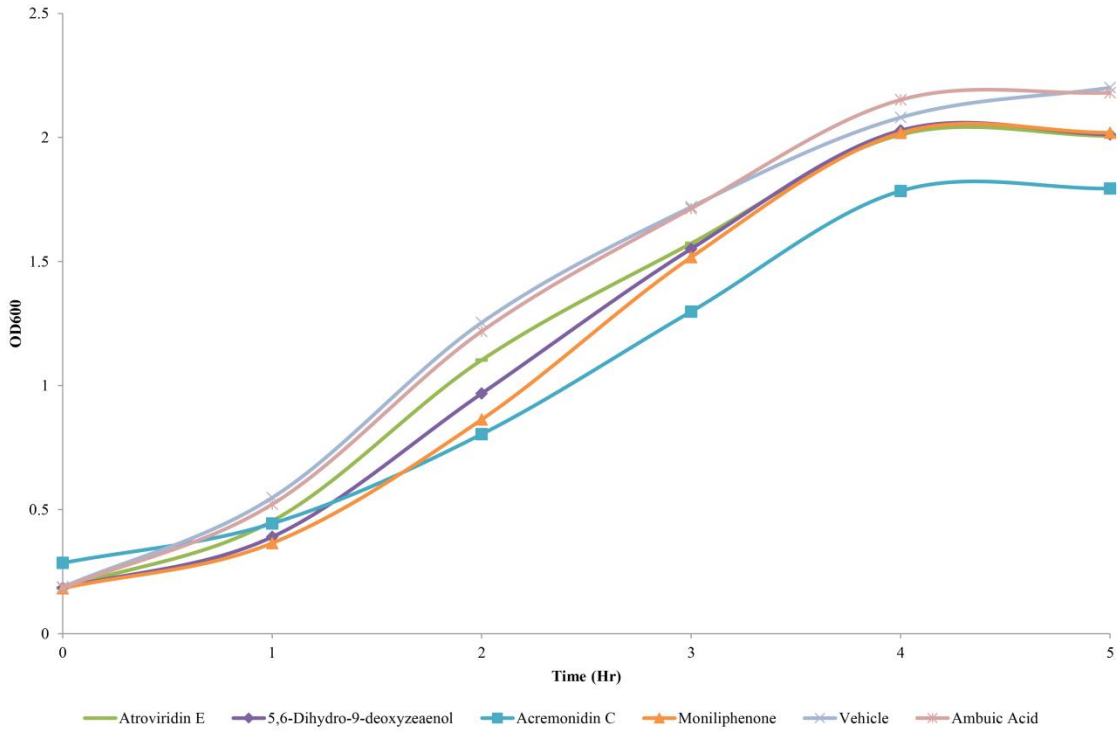


**Figure 16. Growth Curves for Lead Compounds**

Atroviridin E, 5,6-Dihydro-9-deoxyzeaenol, Acremonidin C and Moniliphenone all showed a growth inhibition < 25% and an AIP inhibition > 50%, and were further evaluated.

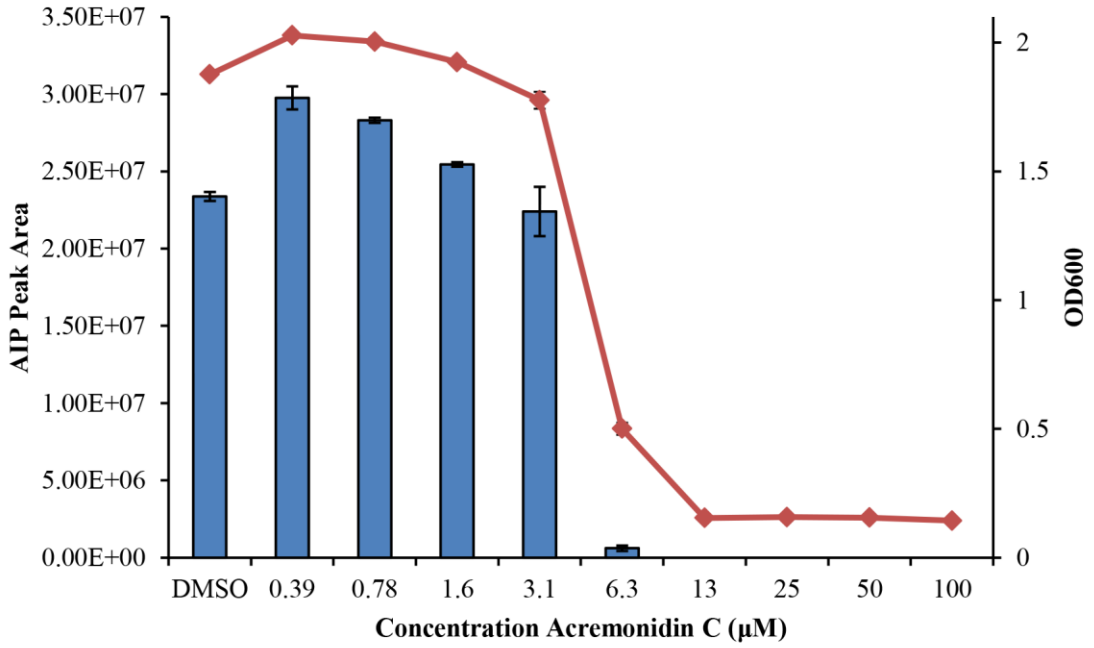


**Figure 17. Evaluation of Acremonidin C**

Acremonidin C showed potential as a lead compound for AIP biosynthesis inhibition and was further evaluated in a dose dependent manner. The endpoint OD600 (red line) was compared to the endpoint AIP peak area (blue bar). It was concluded any AIP inhibition previously observed was a result of growth inhibition.

## 3.4 Discussion

The development of new therapeutics capable of combating bacterial infections through novel mechanisms constitutes a promising strategy for addressing the problem of bacterial resistance. Quorum sensing inhibition has shown promise as a possible mechanism for new therapeutics, and specifically targeting AIP biosynthesis has potential for the development of a broad-spectrum quorum sensing inhibitor. While we were unable to identify any new AIP biosynthesis inhibitors from among the limited selection

of purified natural product compounds screened thus far, we were able to show the potential utility of our novel method as a screening tool for the identification AIP biosynthesis inhibitors, taking a valuable step in the direction of identifying new therapeutic agents.

## 3.5 Conclusion

The engineered strain of *S. aureus* combined with measurements of AIP production facilitated a targeted approach that could be employed in the future for discovering new quorum sensing inhibitors. Utilizing the workflow of our novel bioassay, we are able to efficiently narrow down large libraries of pure compounds to those with potential activity. Our newly developed bioassay can now be used to continue screening libraries of synthetic or natural product compounds, or be utilized by natural product chemists in the bioactivity directed fraction process leading to the discovery of new lead compounds for combating bacterial infections.

# CHAPTER IV

# INDENTIIFACTION OF AN AIP BIOSYNTHESIS INHIBITOR IN GOLDENSEAL (*HYDRASTIS CANADENSIS*) LEAF EXTRACT

## 4.1 Introduction

*Hydrastis canadensis*, goldenseal, is one of the most popular herbal supplements used today [67-69] and is employed as a treatment for a variety of ailments ranging from viral and bacterial infections to intestinal disorders [70, 71]. The alkaloids commonly present in goldenseal extracts are well known for their antimicrobial activity [72, 73], and are often credited for this plant's ability to fight bacterial infections. However, a recent study performed by our lab has demonstrated goldenseal's capability to inhibit of the quorum sensing *agr* system in methicillin-resistant *Staphylococcus aureus* (MRSA) [74]. The benefits of quorum sensing inhibition have previously been described in detail [34] and make it a very enticing mode of action for future therapeutics. It was the goal of this study to investigate the mechanism of action utilized by goldenseal to inhibit the *agr* system and identify the constituents responsible for the observed activity.

The *agr* system in *S. aureus* is reviewed in reference [39] and an overview can be found in Figure 4. While the *agr* system in *S. aureus* is most well-known, several other Gram-positive pathogens containing an *agr* system have been identified. Inhibition of the *agr* system can occur through two pathways, inhibition of the response regulating cascade or inhibition of the AIP biosynthesis system. Inhibitors of AIP biosynthesis have demonstrated the ability to act as broad-spectrum *agr* system inhibitors [50].

Unfortunately, while a number of response regulating inhibitors [33, 51, 59-62] have been identified, only one AIP biosynthesis inhibitor is currently known [50]. Identification of new AIP biosynthesis inhibitors could offer valuable insight into how the *agr* system functions, as well as provide novel compounds for drug leads.

The first goal of this study was to determine if goldenseal plant extract could inhibit the biosynthesis of AIP in *S. aureus.* The second goal of this study was utilize the newly developed assay (Chapter III) combined with bioactivity-directed fraction (Figure 18) to isolate new AIP biosynthesis inhibitors. These newly identified inhibitors could serve as potential leads for future therapeutic development.

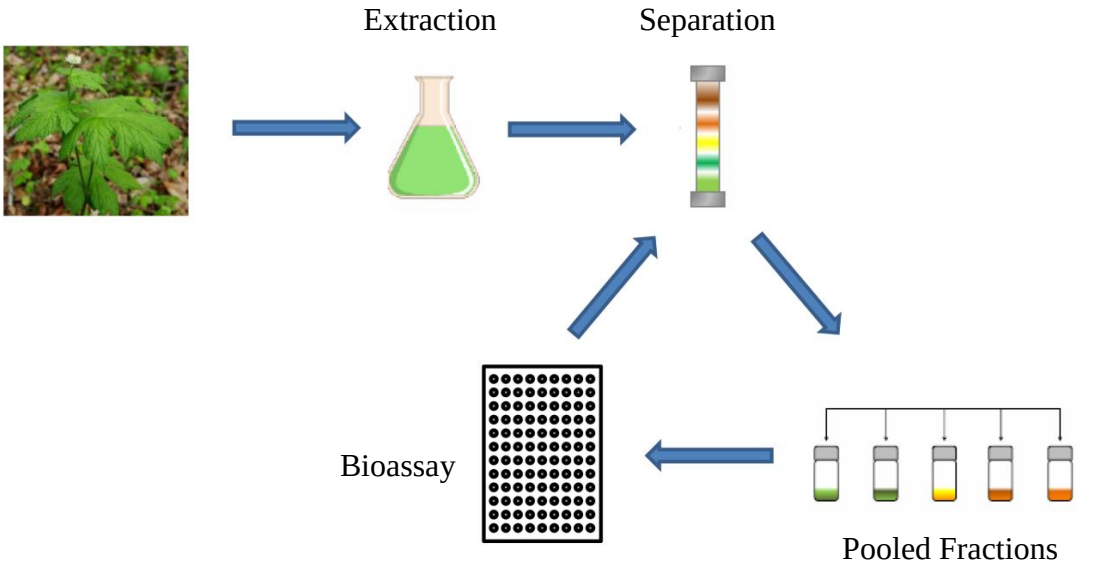


**Figure 18. Overview of Bioactivity-Directed Fractionation**

An organism of interest (plant, fungus, bacteria, etc…) is first extracted and then subjected to chromatographic separation. The eluent is collected in pools and tested for bioactivity. Active pools are subjected to additional chromatographic separation and the resulting pools tested for bioactivity. This process is repeated until the active constituent can be isolated or identified.

## 4.2 Materials and Methods

### 4.2.1 Preparation of a Goldenseal Extract

Goldenseal plant material was harvested from William Burch's farm in Hendersonville, North Carolina (NC, N 35°24.277', W 082°20.993', 702.4 m elevation). A representative voucher specimen (NCU583414) was deposited in the University of North Carolina at Chapel Hill herbarium (NCU). Dried plant material was macerated for a least 24 hr in methanol at a 5:1 ratio (mL of solvent:g of plant material). Extract was separated from plant material using vacuum filtration and then concentrated using rotary evaporation. The methanol extract was combined with equal parts hexanes, and was stirred with a magnetic stir bar for at least one hr. The phases were allowed to separate, and the methanol layer was removed using a separatory funnel. The methanol layer was concentrated using a rotary evaporation, and was partitioned against water and chloroform at a 1:4:5 (methanol:water:chloroform) ratio. Again, phases were allowed to separate and chloroform layer was removed. The chloroform layer was dried using rotary evaporation, and served as the starting material for the subsequent experiments. From this point forward, the chloroform layer will be referred to as the "goldenseal extract".

### 4.2.2 Fractionation of Goldenseal Extract

4.2.2.1 Stages 1 and 2 of Separation

The first two stages of separation have been previously described in detail [75]. In summary, the extract was loaded on a normal-phase silica column and was eluted using automated flash chromatography with a hexane:chloroform:methanol gradient and fractions were collected 1 liter increments. A total of 9 fractions were collected, fractions

1-9. The most active fraction, fraction 2, was subjected to a second stage of separation via flash chromatography utilizing a 120 g silica gel column (RediSep Rf, Teledyne Isco) and a hexane:ethyl acetate:methanol gradient over 50.3 min at a flow rate of 85 mL/min. The resulting fractions were pooled into 13 fractions, fractions 2A-2M, based on UV absorbance profile. Bioactivity of the first two stages of separation was evaluated based on general *agr* system inhibition and method has been previously reported [75].

4.2.2.2 Stage 3 of Separation

The most active fraction, fraction 2C, was test for AgrB inhibition using previously described bioassay (Chapter II). This fraction was active, and therefore was subjected to a third stage of normal-phase chromatography utilizing a 120 g silica gel column (RediSep Rf, Teledyne Isco) and a hexane:ethyl acetate:methanol gradient over 45.2 min at a flow rate of 100 mL/min. Resulting fractions were pooled into 13 pooled fractions, fractions i-xiii, and tested for AIP biosynthesis inhibition (Chapter III).

4.2.2.3 Preparative HPLC

Pooled fractions ii and vii were further purified using reverse-phase preparative HPLC. Samples were eluted from a Gemini-NX 5µ C-18 column (Phenomenex Inc., Torrance, CA) at a flow rate of 21 mL/min using a binary solvent system of acetonitrile (solvent A) and 0.1% acetic acid (solvent B). For fraction ii, the gradient initiated with a five minute isocratic hold at 20:80 (A:B), increased linearly over 20 minutes from 20% A to 100% A, and was held isocratically for 5 min. 48 fractions were collected and pooled into 14 pools based on UV absorbance. Pools were tested for bioactivity.

For fraction vii, the gradient initiated with a five minute isocratic hold at 40:60 (A:B), increased linearly over 50 min from 40% A to 90% A, followed by a 100% A column flush for 10 min. There were 72 fractions collected and pooled into 27 pools, a-aa, based on UV absorbance. Pools were tested for bioactivity and pool i (showing 57% inhibition) was the most active.

Pool i yielded 2.24 mg of material, and was subjected to additional purification using a Synergi 4µ Max-RP column at a flow rate of 4.72 mL/min. The gradient initiated with a 5 min isocratic hold of 30:70 (A:B), increased to 40% A over 0.1 min, increased linearly from 40% A to 50% A over 20 min, and column was flushed with 100% A for 10 minutes. A total of ten fractions were collected and pooled into 8 pools. Pool 4 eluted from the column between 14.00-19.09 min, and yielded 1.01 mg of 80% pure material (**1**) at 16.1 min. All other fractions were too complex and low yielding to identify constituents.

### 4.2.3 Identification of 8-Oxotetrahydrothalifendine

Pooled fraction 4 was analyzed using liquid chromatography-mass spectrometry (LC-MS) performed on an Aquity ultra-high performance liquid chromatography (UPLC) system (Waters Corporation, Milford, MA) coupled to a LTQ Orbitrap XL hybrid mass spectrometer (Thermo Fisher Scientific, Waltham, MA). An ion with an *m/z* value of 340.1172 and UV $\lambda_{max}$ 200, 216, 293 nm was identified as the primary constituent of this pool. These values corresponded to a previously identified constituent of goldenseal, 8-oxotetrahydrothalifendine (calc. *m/z* 340.1185, reported UV $\lambda_{max}$ 207, 217, 291) [76]. A sample of compound 1 (purity >90%) was reisolated from a second batch of *H.*

*canadensis* leaves, and identity was confirmed using LC-MS and $^{1}$H NMR obtained using a JOEL ECS 400 MHz NMR spectrometer.

### 4.2.4 AIP Biosynthesis Inhibition Assay

The isolated 8-oxotetrahydrothalifendine (purity > 90%) was tested for AIP biosynthesis inhibition using a previously described bioassay (Chapter II). Briefly, an overnight culture of AIP constitutively producing strain (AH2989), see Chapter III, was diluted 1:200 (culture:broth) and shaken (200 rpm) at 37 °C for two hr. The bacteria culture (200 μL) was combined with 45 μL broth and 5 μL dimethyl sulfoxide (DMSO) containing 8-oxotetrahydrothalifendine in concentrations of 500 μM and 5 mM. Final concentration of 8-oxotetrahydrothalifendine in culture was 10 μM and 100 μM, respectively. Cultures were shaken at 1000 rpm at 37 °C using a Stuart S1505 microtitre plate shaker (Bibby Scientific Limited, Staffordshire, U.K.). An optical density of 600 nm was used to monitor cell growth at one hr intervals. Cells were grown to the end of the log-phase and were removed via vacuum filtration. Filtrate was analyzed using LC-MS parameters described in 2.2.4. Selected ion chromatograms for *m/z* value 961.3788 were plotted and peak area values were used for relative AIP concentration comparison.

## 4.3 Results

The fourth round of bioactivity-guide fractionation of the goldenseal extract resulted in two active fractions (fractions ii and vii) with an inhibition of 56% and 41% respectively (Figure 19). Further evaluation of fraction ii showed the observed decrease in AIP production was due to growth inhibition, and therefore no further experiments were pursued with this fraction. However, fraction vii showed no significant growth

effect and was further purified (Figure 20), resulting in the identification of 8-oxotetrahydrothalifendine **(1)** as an AIP biosynthesis inhibitor. This compound has previously been identified as a constituent of goldenseal [76], however, no bioactivity has been reported. Compound **1** was re-isolated from a scaled up extract, and a comparison of the accurate mass LC-MS chromatograms for the purified 8-oxotetrahydrothalifendine, fraction i, and the final pool 4 confirmed the correct compound was re-isolated (Figure 21).

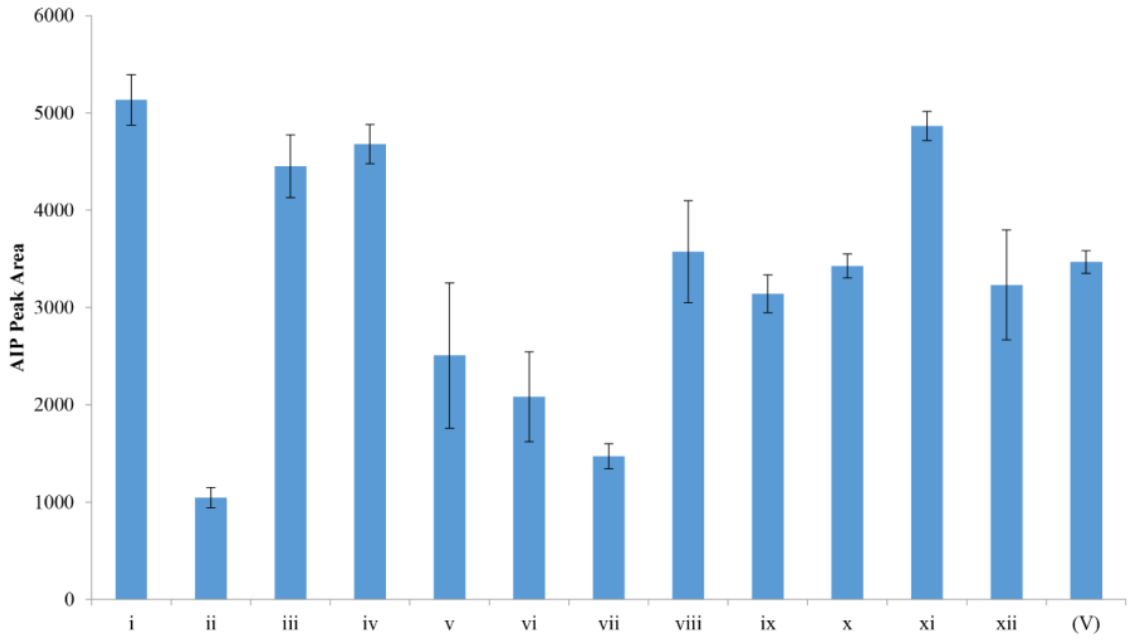


**Figure 19. Bioactivity of Fractions i-xii**

Fractions i-xii were tested for AIP biosynthesis inhibition. The vehicle control (V) consisted of 2% DMSO in broth. The most active fractions, ii and vii, were subjected to additional purification steps.

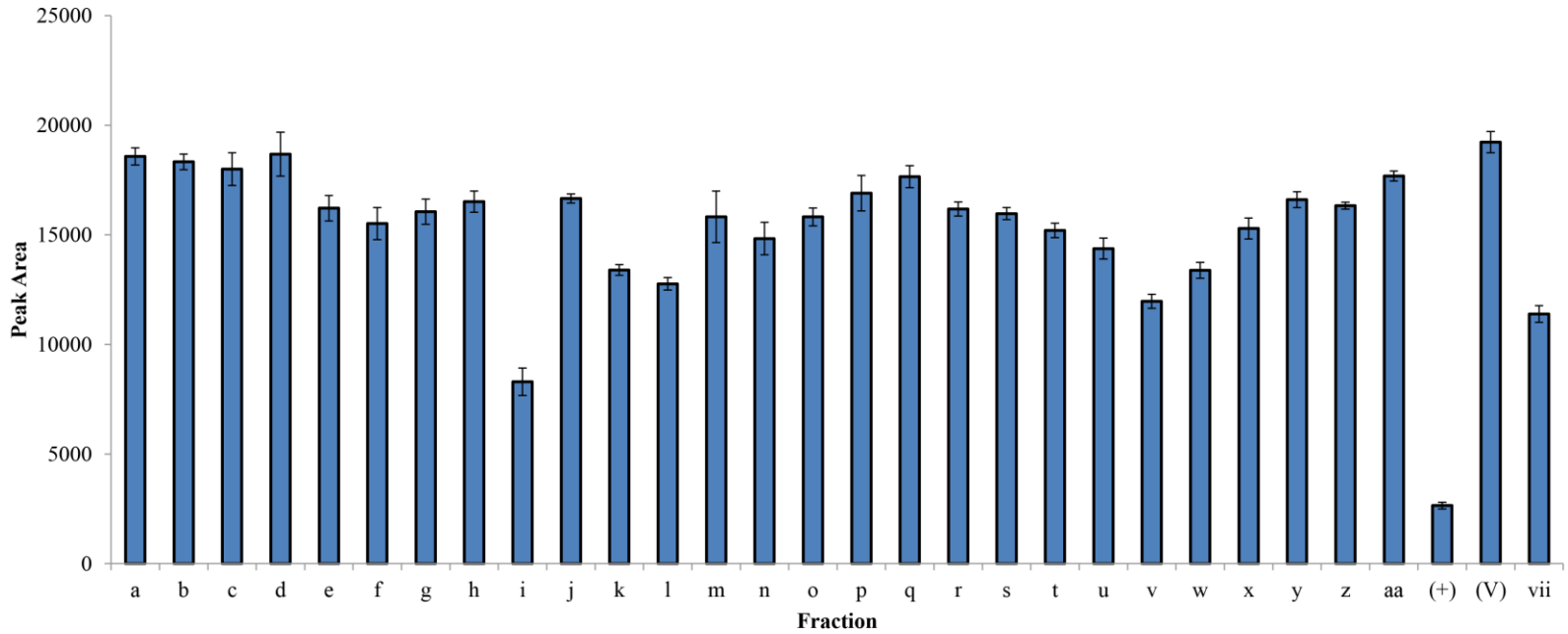


**Figure 20. Bioactivity of Fractions a-aa**

Fractions a-aa, collected from fraction vii, were tested for AIP biosynthesis inhibition. Ambuic acid (50 μM) was used as a positive control (+) to ensure proper biological response was being observed, and fraction vii (the starting material) was tested to ensure activity wasn't lost.

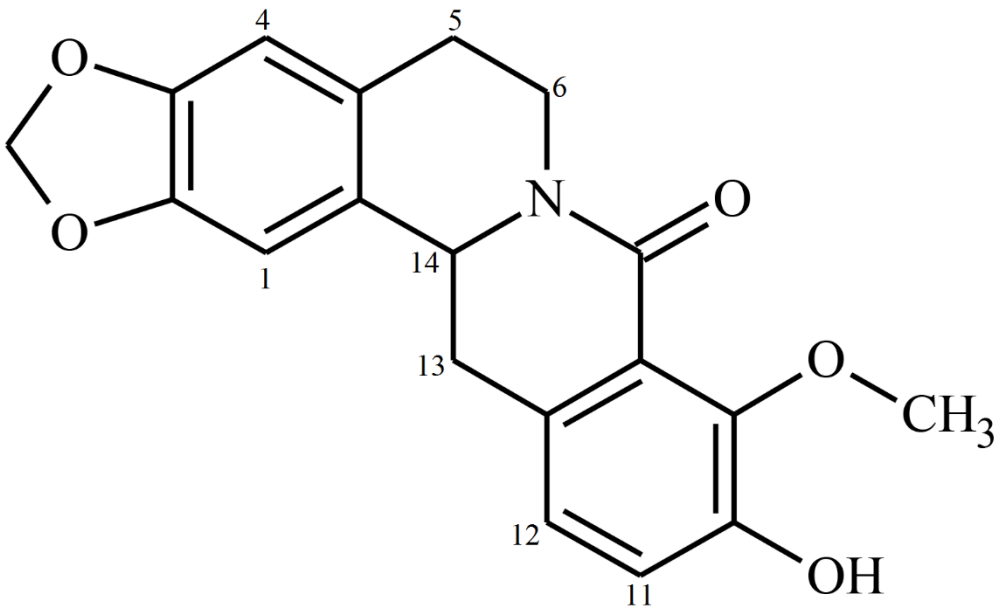


**(1)**

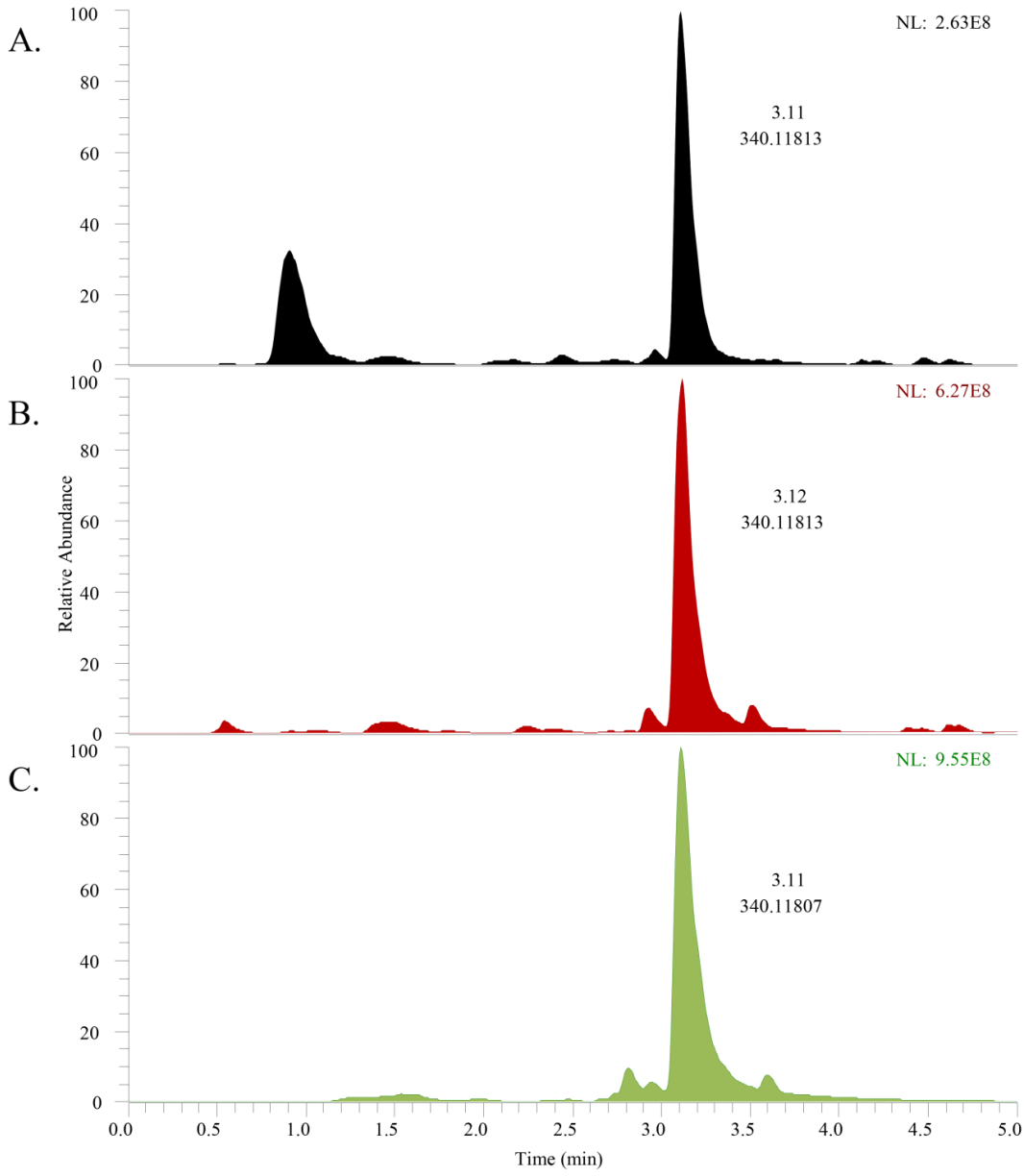


**Figure 21. Confirmation of 8-Oxotetrahydrothalifendine in Fractions.**

The base peak chromatograms for fraction i (A), pool 4 (B), and purified 8-oxotetrahydrothalifendine (C) indicating 8-oxotetrahydrothalifendine as the primary constituent of the active fractions. Indicated on each chromatogram is the retention time for the observed peak and the *m/z* value observed at that time. The signal intensity used for normalization (NL) is also indicated in the upper right corner of each chromatogram.

Previously published $^{1}$H NMR shifts for 8-oxotetrahydrothalifendine [77] and the calculated accurate mass (*m/z* 340.1185) were used to confirm the identity of compound 1 (Table 5). 8-oxotetrahydrothalifendine displays very weak potency ($IC_{50}$ >100 μM) (Figure 22) as an AIP biosynthesis inhibitor, however, it is only the second known compound to inhibit the *agr* system through this unique mode of action. The identification of this compound may help provide valuable insight into the *agr* system, as well as serve as template for future drug design.

**Table 5. Comparison of Experimental and Literature NMR Values for 8-Oxotetrahydrothalifendine**

| Position | $\delta_H$, M (J in Hz) experimental | $\delta_H$, M (J in Hz) literature [77] |
|---|---|---|
| 1 | 6.65 | 6.67 |
| 4 | 6.67 | 6.68 |
| 5 ax | 2.90 (13.9,11.1) | 2.89 (15,11,3) |
| 5 eq | 2.75 (14.9,3.3,2) | 2.75 (15,3,2) |
| 6 ax | 2.94 (12.1,11.5,2.5) | 2.95 (12.5,11,2.5) |
| 6 eq | 4.95 (m) | 4.97 (m) |
| 11 | 7.06 (8.2) | 7.07 (8) |
| 12 | 6.89 (8.2) | 6.90 (8) |
| 13a | 3.00 (15.3,3.4) | 3.02 (15.5,3) |
| 13b | 2.85 (15.2,13.6) | 2.84 (15.5,13.5) |
| 14 | 4.72 (13.3,2.8) | 4.73 |
| OMe | 3.99 | 4.01 |
| OH | 6.03 | 6.03 |
| O-$CH_2$-O | 5.95 | 5.96 |

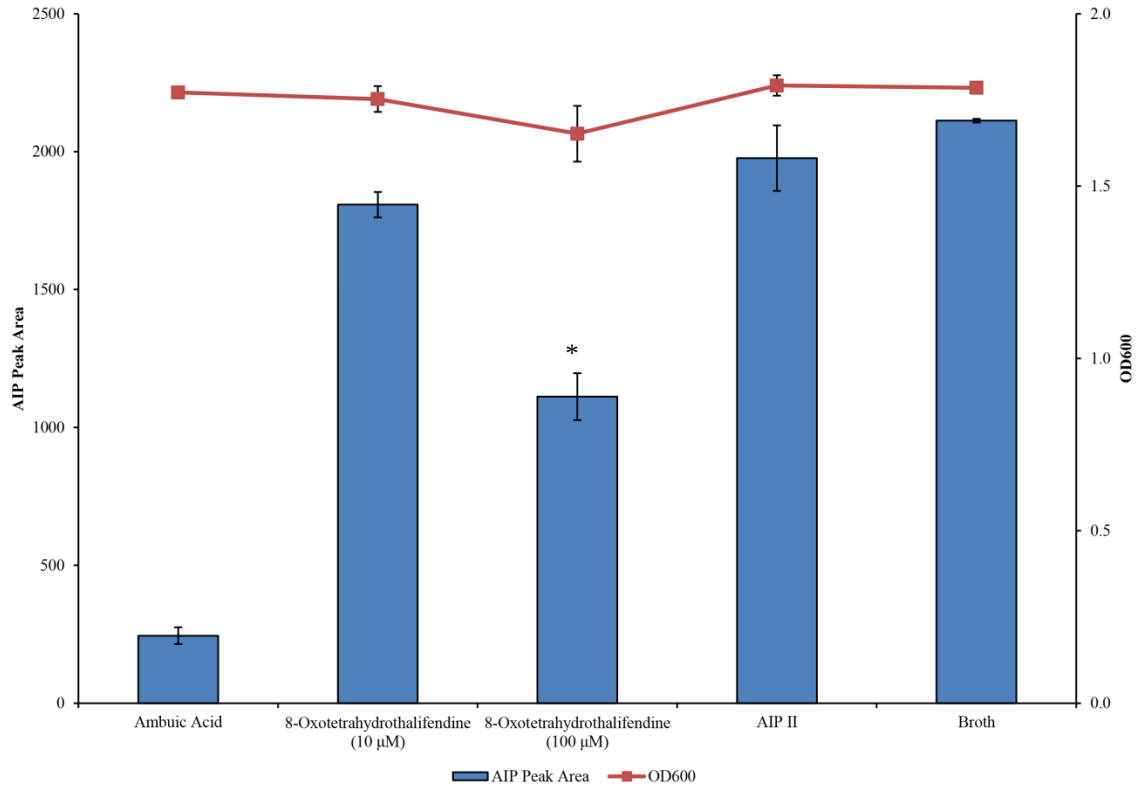


**Figure 22. Bioactivity of 8-Oxotetrahydrothalifendine.**

AIP peak area is represented by the blue bars, and OD600 is represented by the red line. Ambuic acid was used as a positive control that shows AIP biosynthesis inhibition while having no effect on growth. Since the AIP constitutively producing strain (AH2989) was used for screening, AIP II, a known AgrC inhibitor, should have no effect on the AIP production. 8-Oxotetrahydrothalifendine was tested for AIP biosynthesis inhibition at two concentrations (10 µM and 100 µM). While 10 µM showed no inhibition, 100 µM 8-oxotetrahydrothalifendine inhibited AIP biosynthesis by 49% (*$p < 0.001$).

## 4.4 Discussion

Previously published studies have demonstrated capability of a goldenseal extract to inhibit the *agr* system in *S. aureus* [74], and it was the goal of this study to further investigate this inhibition and identify the active constituents. While goldenseal extract

may inhibit the *agr* system through multiple modes of action, our newly developed bioassay (Chapter II) showed it does, in part, work through the inhibition AIP biosynthesis. This mode of action is very unique, with only one known AIP biosynthesis inhibitor previously published [50]. Importantly, signal biosynthesis inhibition has the potential for development of a broad-spectrum therapeutic against Gram-positive bacterial pathogens (Chapter I).

Through the results presented here, we were able to identify a new AIP biosynthesis inhibitor, 8-oxotetrahydrothalifendine; however, the activity of this compound does not fully explain the AgrB inhibition observed from its initial fraction, fraction vii. Unfortunately, we were unable to pursue further purification of the additional fractions collected due to limitations in quantity of material available for isolation (< 1mg).

## 4.5 Conclusion

AgrB inhibition is a novel approach for combating Gram-positive bacterial pathogens, and this study shows the potential benefit of utilizing our newly developed targeted assay for the identification of AIP biosynthesis inhibitors. The newly discovered AgrB inhibitor, 8-oxotetrahydrothalifendine, will be the subject of future studies that evaluate its potential broad-spectrum activity, and this compound may serve as a lead for the development of future anti-virulence therapeutics.

# CHAPTER V

# CONCLUDING THOUGHTS AND COMMENTS

The problem of antibiotic resistant bacteria has placed a serious burden on the well-being of world's healthcare systems. This has many healthcare professionals warning that without immediate intervention we will enter a "post-antibiotic" era, in which simple cuts, scraps and burns could result in deadly bacterial infections [78]. Anti-virulence has emerged as a potential strategy for combating bacterial pathogens. When tested in animal models, anti-virulence compounds have significantly reduced the effect of bacterial infections and have proven to be less susceptible to resistance development [33]. Unfortunately, while anti-virulence has shown promise as a therapeutic strategy, no compounds have been approved for clinical use. The majority of *agr* system inhibitors are antagonist peptides, however, as previously stated AgrC is highly susceptible to mutation. Inhibitors of the AgrA and AgrB may be the best candidates for therapeutic development, unfortunately only a limited number of compounds showing these actives have been discovered and their potency is very limited. Thus, there is a need for additional therapeutic leads capable of inhibiting either AgrA or AgrB.

The studies presented here explored the *agr* system and developed a new assay for identifying *agr* system inhibitors. Chapter II presented a method for identifying and detecting AIP, the *agr* regulator, in the growth media of multiple species of bacteria. Using this knowledge, we were able to monitor *agr* system activity in each of these

species. Traditional methods for monitoring *agr* system activity relied on the development of bioengineered strains of each species of bacteria to serve as a representative model. Our method allows for a direct evaluation of the clinically relevant strain. In Chapter III, we explored a target for broad-spectrum *agr* inhibition, AIP biosynthesis, and provided a novel screening assay for the identification of compounds that specifically target AIP biosynthesis. This screening method can now be used to efficiently screen libraries of known compounds to discover new drug leads. We also incorporated our novel screening method in to the bioactivity-guide fractionation process utilized in traditional natural products, Chapter IV. This allowed us to identify 8-oxotetrahydrothalifendine, a known constituent of the medicinal plant goldenseal, as an AIP biosynthesis inhibitor. While 8-oxotetrahydrothalifendine wasn't a very potent inhibitor, it did validate the approach using our novel assay. Moving forward our assay will be used to screen multiple pure compound and natural product extract libraries for potential drug leads that inhibit signal biosynthesis.

REFERENCES


1. R. I. Aminov, A brief history of the antibiotic era: lessons learned and challenges for the future. *Front Microbiol* **1**, 134 (2010).

2. D. Charles, B. Larsen, Streptococcal puerperal sepsis and obstetric infections: a historical perspective. *Reviews of Infectious Diseases* **8**, 411-422 (1986).

3. K. E. Nelson, C. M. Williams, *Infectious disease epidemiology : theory and practice*. (Jones and Bartlett Publishers, Sudbury, Mass., 2007).

4. J. H. Powers, Antimicrobial drug development--the past, the present, and the future. *Clin Microbiol Infect* **10 Suppl 4**, 23-31 (2004).

5. A. Fleming, On the antibacterial action of cultures of a peniccilium, with special reference to their use in the isolation of *b. influenze*. *Bulletin of the World Health Organization* **79**, 780-780 (2001).

6. E. Chain, The classic: penicillin as a chemotherapeutic agent. 1940. *Clinical Orthopaedics and Related Research* **439**, 23-26 (2005).

7. C. M. Grossman, The first use of penicillin in the United States. *Ann Intern Med* **149**, 135-136 (2008).

8. "889 Nobel Laureates since 1901, awarded for "the benefit on mankind"," www.nobelprize.org (accessed May 18).

9. A. Schatz, E. Bugie, S. A. Waksman, Streptomycin, a substance exhibiting antibiotic activity against gram-positive and gram-negative bacteria. 1944. *Clin Orthop Relat Res*, 3-6 (2005).

10. M. Wainwright, *Miracle cure : the story of penicillin and the golden age of antibiotics*. (Blackwell, Oxford, UK ; Cambridge, Mass., USA, 1990).

11. C. L. Moberg, Z. Cohn, *Launching the antibiotic era : personal accounts of the discovery and use of the first antibiotics*. (Rockefeller University Press, New York, 1990).

12. S. K. Sahni, H. P. Narra, A. Sahni, D. H. Walker, Recent molecular insights into rickettsial pathogenesis and immunity. *Future Microbiol* **8**, 1265-1288 (2013).

13. C. Walsh, Where will new antibiotics come from? *Nat Rev Microbiol* **1**, 65-70 (2003).

14. L. L. Silver, Challenges of antibacterial discovery. *Clin Microbiol Rev* **24**, 71-109 (2011).

15. C. R. Friedman, C. G. Whitney, It's time for a change in practice: reducing antibiotic use can alter antibiotic resistance. *J Infect Dis* **197**, 1082-1083 (2008).

16. R. Gonzales, D. C. Malone, J. H. Maselli, M. A. Sande, Excessive antibiotic use for acute respiratory infections in the United States. *Clin Infect Dis* **33**, 757-762 (2001).

17. "Antibiotic resistance threats in the United States, 2013," Centers for Disease Control and Prevention Report ar-threats-2013-508 (2013).

18. D. A. Kessler, Antibiotics and the meat we eat. *New York Times* **162**, (2013).

19. B. M. Marshall, S. B. Levy, Food animals and antimicrobials: impacts on human health. *Clin Microbiol Rev* **24**, 718-733 (2011).

20. R. S. Singer, J. Williams-Nguyen, Human health impacts of antibiotic use in agriculture: A push for improved causal inference. *Curr Opin Microbiol* **19**, 1-8 (2014).

21. L. M. Durso, K. L. Cook, Impacts of antibiotic use in agriculture: what are the benefits and risks? *Curr Opin Microbiol* **19**, 37-44 (2014).

22. J. Davies, D. Davies, Origins and evolution of antibiotic resistance. *Microbiol Mol Biol Rev* **74**, 417-433 (2010).

23. H. Heuer, H. Schmitt, K. Smalla, Antibiotic resistance gene spread due to manure application on agricultural fields. *Curr Opin Microbiol* **14**, 236-243 (2011).

24. S. Borràs *et al.*, Analysis of antimicrobial agents in animal feed. *TrAC Trends in Analytical Chemistry* **30**, 1042-1064 (2011).

25. E. P. Abraham, E. Chain, An enzyme from bacteria able to destroy penicillin. 1940. *Rev Infect Dis* **10**, 677-678 (1988).

26. C. Walsh, *Antibiotics : actions, origins, resistance*. (ASM Press, Washington, D.C., 2003).

27. D. Lim, N. C. Strynadka, Structural basis for the beta lactam resistance of PBP2a from methicillin-resistant Staphylococcus aureus. *Nat Struct Biol* **9**, 870-876 (2002).

28. J. Sun, Z. Deng, A. Yan, Bacterial multidrug efflux pumps: mechanisms, physiology and pharmacological exploitations. *Biochem Biophys Res Commun* **453**, 254-267 (2014).

29. K. Bhullar *et al.*, Antibiotic resistance is prevalent in an isolated cave microbiome. *PLoS One* **7**, e34953 (2012).

30. G. P. Tegos *et al.*, Microbial efflux pump inhibition: tactics and strategies. *Curr Pharm Des* **17**, 1291-1302 (2011).

31. O. Lomovskaya *et al.*, Identification and characterization of inhibitors of multidrug resistance efflux pumps in *Pseudomonas aeruginosa*: novel agents for combination therapy. *Antimicrob Agents Chemother* **45**, 105-116 (2001).

32. D. A. Rasko, V. Sperandio, Anti-virulence strategies to combat bacteria-mediated disease. *Nat Rev Drug Discov* **9**, 117-128 (2010).

33. E. K. Sully *et al.*, Selective chemical inhibition of agr quorum sensing in *Staphylococcus aureus* promotes host defense with minimal impact on resistance. *PLoS Pathog* **10**, e1004174 (2014).

34. N. B. Cech, A. R. Horswill, Small-molecule quorum quenchers to prevent *Staphylococcus aureus* infection. *Future Microbiol* **8**, 1511-1514 (2013).

35. J. S. Wright, R. Jin, R. P. Novick, Transient interference with staphylococcal quorum sensing blocks abscess formation. *Proc Natl Acad Sci U S A* **102**, 1691-1696 (2005).

36. B. Gray, P. Hall, H. Gresham, Targeting *agr*- and *agr*-Like quorum sensing systems for development of common therapeutics to treat multiple gram-positive bacterial infections. *Sensors (Basel)* **13**, 5130-5166 (2013).

37. X. Qin, K. V. Singh, G. M. Weinstock, B. E. Murray, Effects of *Enterococcus faecalis fsr* genes on production of gelatinase and a serine protease and virulence. *Infect Immun* **68**, 2579-2586 (2000).

38. D. Garmyn, L. Gal, J. P. Lemaitre, A. Hartmann, P. Piveteau, Communication and autoinduction in the species *Listeria monocytogenes*: A central role for the *agr* system. *Commun Integr Biol* **2**, 371-374 (2009).

39. M. Thoendel, J. S. Kavanaugh, C. E. Flack, A. R. Horswill, Peptide signaling in the staphylococci. *Chem Rev* **111**, 117-151 (2011).

40. C. P. Gordon, P. Williams, W. C. Chan, Attenuating *Staphylococcus aureus* virulence gene regulation: a medicinal chemistry perspective. *J Med Chem* **56**, 1389-1404 (2013).

41. G. Ji, R. C. Beavis, R. P. Novick, Cell density control of staphylococcal virulence mediated by an octapeptide pheromone. *Proc Natl Acad Sci U S A* **92**, 12055-12059 (1995).

42. J. Nakayama *et al.*, Gelatinase biosynthesis-activating pheromone: a peptide lactone that mediates a quorum sensing in *Enterococcus faecalis*. *Mol Microbiol* **41**, 145-154 (2001).

43. P. MDowell *et al.*, Structure, activity and evolution of the group I thiolactone peptide quorum-sensing system of *Staphylococcus aureus*. *Mol Microbiol* **41**, 503-512 (2001).

44. M. E. Olson *et al.*, *Staphylococcus epidermidis agr* quorum-sensing system: signal identification, cross talk, and importance in colonization. *J Bacteriol* **196**, 3482-3493 (2014).

45. M. Kalkum, G. J. Lyon, B. T. Chait, Detection of secreted peptides by using hypothesis-driven multistage mass spectrometry. *Proc. Natl. Acad. Sci. U. S. A.* **100**, 2795-2800 (2003).

46. H. A. Junio *et al.*, Quantitative analysis of autoinducing peptide I (AIP-I) from *Staphylococcus aureus* cultures using ultrahigh performance liquid chromatography-high resolving power mass spectrometry. *J Chromatogr B Analyt Technol Biomed Life Sci* **930**, 7-12 (2013).

47. P. Glaser *et al.*, Comparative genomics of *Listeria* species. *Science* **294**, 849-852 (2001).

48. A. F. Gillaspy *et al.*, Role of the accessory gene regulator (*agr*) in pathogenesis of staphylococcal osteomyelitis. *Infect Immun* **63**, 3373-3380 (1995).

49. R. P. Novick, T. W. Muir, Virulence gene regulation by peptides in staphylococci and other Gram-positive bacteria. *Current Opinion in Microbiology* **2**, 40-45 (1999).

50. J. Nakayama *et al.*, Ambuic acid inhibits the biosynthesis of cyclic peptide quormones in Gram-positive bacteria. *Antimicrobial Agents and Chemotherapy* **53**, 580-586 (2009).

51. E. J. Murray *et al.*, Targeting *Staphylococcus aureus* quorum sensing with nonpeptidic small molecule inhibitors. *J Med Chem* **57**, 2813-2819 (2014).

52. P. Buzder-Lantos, K. Bockstael, J. Anné, P. Herdewijn, Substrate based peptide aldehyde inhibits bacterial type I signal peptidase. *Bioorg Med Chem Lett* **19**, 2880-2883 (2009).

53. S. E. Desouky *et al.*, High-throughput screening of inhibitors targeting *agr*/*fsr* quorum sensing in *Staphylococcus aureus* and *Enterococcus faecalis*. *Biosci Biotechnol Biochem* **77**, 923-927 (2013).

54. M. Otto, R. Sussmuth, C. Vuong, G. Jung, F. Gotz, Inhibition of virulence factor expression in *Staphylococcus aureus* by the *Staphylococcus epidermidis agr* pheromone and derivatives. *Febs Letters* **450**, 257-262 (1999).

55. M. Otto, H. Echner, W. Voelter, F. Götz, Pheromone cross-inhibition between *Staphylococcus aureus* and *Staphylococcus epidermidis*. *Infect Immun* **69**, 1957-1960 (2001).

56. T. Iwase *et al.*, Staphylococcus epidermidis Esp inhibits *Staphylococcus aureus* biofilm formation and nasal colonization. *Nature* **465**, 346-349 (2010).

57. F. A. Ferreira *et al.*, Impact of agr dysfunction on virulence profiles and infections associated with a novel methicillin-resistant *Staphylococcus aureus* (MRSA) variant of the lineage ST1-SCCmec IV. *BMC Microbiol* **13**, 93 (2013).

58. C. L. Quave, A. R. Horswill, Flipping the switch: tools for detecting small molecule inhibitors of staphylococcal virulence. *Front Microbiol* **5**, 706 (2014).

59. W. C. Chan, B. J. Coyle, P. Williams, Virulence regulation and quorum sensing in staphylococcal infections: competitive AgrC antagonists as quorum sensing inhibitors. *J Med Chem* **47**, 4633-4641 (2004).

60. E. A. George, R. P. Novick, T. W. Muir, Cyclic peptide inhibitors of staphylococcal virulence prepared by Fmoc-based thiolactone peptide synthesis. *J Am Chem Soc* **130**, 4914-4924 (2008).

61. P. G. Leonard, I. F. Bezar, D. J. Sidote, A. M. Stock, Identification of a hydrophobic cleft in the LytTR domain of AgrA as a locus for small molecule interactions that inhibit DNA binding. *Biochemistry* **51**, 10035-10043 (2012).

62. V. Khodaverdian *et al.*, Discovery of antivirulence agents against methicillin-resistant *Staphylococcus aureus*. *Antimicrob Agents Chemother* **57**, 3645-3652 (2013).

63. G. A. Somerville *et al.*, In vitro serial passage of *Staphylococcus aureus*: changes in physiology, virulence factor production, and agr nucleotide sequence. *J Bacteriol* **184**, 1430-1437 (2002).

64. B. R. Boles, M. Thoendel, A. J. Roth, A. R. Horswill, Identification of genes involved in polysaccharide-independent *Staphylococcus aureus* biofilm formation. *PLoS One* **5**, e10146 (2010).

65. M. R. Kiedrowski *et al.*, Nuclease modulates biofilm formation in community-associated methicillin-resistant *Staphylococcus aureus*. *PLoS One* **6**, e26714 (2011).

66. T. T. Luong, C. Y. Lee, Improved single-copy integration vectors for *Staphylococcus aureus*. *J Microbiol Methods* **70**, 186-190 (2007).

67. H. A. Junio *et al.*, Synergy-directed fractionation of botanical medicines: a case study with goldenseal (*Hydrastis canadensis*). *J Nat Prod* **74**, 1621-1629 (2011).

68. "Herbal Supplements, Prescription Drugs, Rx-to-OTC Products," B. R. Report 202 (2006).

69. P. Barnes, E. Powell-Griner, K. McFann, R. Nahin, *CDC Advance Data Report* **343**, 1-24 (2004).

70. R. Upton, Goldenseal root *(Hydrastis Canadensis). Standards of Analysis, Quality Control and Therapeutics*, (2001).

71. K. Abascal, E. Yarnell, Combining herbs in a formula for irritable bowel syndrome. *Alternative and Complementary Therapies* **11**, 17-23 (2005).

72. C. L. Kuo, C. W. Chi, T. Y. Liu, The anti-inflammatory potential of berberine in vitro and in vivo. *Cancer Lett* **203**, 127-137 (2004).

73. Y. Li, G. Y. Zuo, Advances in studies on antimicrobial activities of alkaloids. *Chinese Traditional and Herbal Drugs* **41**, 1006-1014 (2010).

74. N. B. Cech, H. A. Junio, L. W. Ackermann, J. S. Kavanaugh, A. R. Horswill, Quorum quenching and antimicrobial activity of goldenseal (*Hydrastis canadensis*) against methicillin-resistant *Staphylococcus aureus* (MRSA). *Planta Medica* **78**, 1556-1561 (2012).

75. K. A. Ettefagh, Inhibiting antimicrobial resistance in *Staphylococcus aureus* using natural products. dissertation, University of North Carolina at Greensboro (2013).

76. E. J. Gentry *et al.*, Antitubercular natural products: berberine from the roots of commercial *Hydrastis canadensis* powder. Isolation of inactive 8-oxotetrahydrothalifendine, canadine, beta-hydrastine, and two new quinic acid esters, hycandinic acid esters-1 and -2. *J Nat Prod* **61**, 1187-1193 (1998).

77. P. M. M. Pinho *et al.*, Protoberberine alkaloids from *Coscinium fenestratum*. *Phytochemistry* **31**, 1403-1407 (1992).

78. "Antimicrobial resistance: global report on surveillance 2014," World Health Organization Report. ISBN: 978 92 4 156474 8 (2014).